Life in an Arsenic-Containing Gold Mine: Genome and Physiology of the Autotrophic Arsenite-Oxidizing Bacterium *Rhizobium* sp. NT-26

Jérémy Andres[1], Florence Arsène-Ploetze[1], Valérie Barbe[2], Céline Brochier-Armanet[3], Jessica Cleiss-Arnold[1], Jean-Yves Coppée[4], Marie-Agnès Dillies[4], Lucie Geist[1], Aurélie Joublin[1], Sandrine Koechler[1], Florent Lassalle[3,5,6], Marie Marchal[1], Claudine Médigue[7], Daniel Muller[6], Xavier Nesme[6], Frédéric Plewniak[1], Caroline Proux[4], Martha Helena Ramírez-Bahena[6,8], Chantal Schenowitz[2], Odile Sismeiro[4], David Vallenet[7], Joanne M. Santini[5,*], and Philippe N. Bertin[1,*]

[1]Laboratoire Génétique Moléculaire, Génomique et Microbiologie, UMR7156 CNRS Université de Strasbourg, Strasbourg, France

[2]Laboratoire de Finition, CEA-IG-Genoscope, Evry, France

[3]Université de Lyon, Université Lyon 1, CNRS, Laboratoire de Biométrie et Biologie Evolutive, UMR5558, Villeurbanne, France

[4]Plate-forme Technologique Transcriptome et Epigénome, Institut Pasteur, Paris, France

[5]Institute of Structural and Molecular Biology, University College London, United Kingdom

[6]Université de Lyon, Université Lyon 1, CNRS, INRA, Laboratoire Ecologie Microbienne Lyon, UMR5557, USC1193, Villeurbanne, France

[7]Laboratoire Analyses Bioinformatiques pour la Génomique et le Métabolisme, Genoscope-IG-CEA, Evry, France

[8]Instituto de Recursos Naturales y Agrobiologia, IRNASA-CSIC, Salamanca, Spain

*Corresponding authors: E-mail: philippe.bertin@unistra.fr; j.santini@ucl.ac.uk.

Abstract

Arsenic is widespread in the environment and its presence is a result of natural or anthropogenic activities. Microbes have developed different mechanisms to deal with toxic compounds such as arsenic and this is to resist or metabolize the compound. Here, we present the first reference set of genomic, transcriptomic and proteomic data of an *Alphaproteobacterium* isolated from an arsenic-containing goldmine: *Rhizobium* sp. NT-26. Although phylogenetically related to the plant-associated bacteria, this organism has lost the major colonizing capabilities needed for symbiosis with legumes. In contrast, the genome of *Rhizobium* sp. NT-26 comprises a megaplasmid containing the various genes, which enable it to metabolize arsenite. Remarkably, although the genes required for arsenite oxidation and flagellar motility/biofilm formation are carried by the megaplasmid and the chromosome, respectively, a coordinate regulation of these two mechanisms was observed. Taken together, these processes illustrate the impact environmental pressure can have on the evolution of bacterial genomes, improving the fitness of bacterial strains by the acquisition of novel functions.

Key words: arsenic metabolism, motility/biofilm, *Rhizobium/Agrobacterium*, transcriptomics/proteomics, phylogeny, rhizosphere.

Introduction

To deal with high concentrations of toxic metals, microorganisms have evolved various strategies, which enable them to detoxify their environment. These processes involve physicochemical reactions, for example, precipitation or solubilization, adsorption or desorption (Borch et al. 2010), and metabolic oxido-reduction reactions (Gadd 2010). In addition, most of the metallic elements found in the periodic table may play a crucial role in microbial physiology, for example, as components of metalloproteins, or as electron

donors or acceptors in energy metabolism (Stolz 2011). Such a metabolism may have been important in the early stages of life, due to a high concentration of metals, including arsenic, in the primordial planet (reviewed in van Lis et al. 2012).

In recent years, the various "omics" methods, which include genome sequencing, comparative genomics, and transcriptome or proteome analysis, have allowed to address the physiology of organisms in a global way. Such approaches have therefore greatly improved the understanding of microbial metabolism (Bertin et al. 2008; Holmes et al. 2009; Wilkins et al. 2009), including the global functioning of ecosystems, as recently demonstrated for an arsenic-rich microbial community (Bertin et al. 2011). To date, the genomes of more than 20 arsenic-metabolizing strains have been sequenced. They originate from various environments, belong to unrelated taxonomic groups, and have different carbon and energy requirements (reviewed in Bertin et al. 2012; van Lis et al. 2013).

Regarding arsenic, which is mainly present in two oxidation states in aquatic environments, that is, arsenite [As(III)] and arsenate [As(V)], microorganisms have acquired various metabolic capacities. These include As(V) reduction, which is usually part of the resistance mechanism, but also functions involved in As(III) oxidation or methylation (reviewed in Stolz 2011). Unlike arsenite methyltransferase genes, which are not often found in bacterial genomes, genes encoding arsenite oxidase are widespread in Bacteria and Archaea (Heinrich-Salmeron et al. 2011 and reviewed in Osborne and Santini 2012). In Herminiimonas arsenicoxidans, the arsenite oxidase aioBA genes are located in an arsenic genomic island, which also contains genes involved in arsenic resistance and biosynthesis of a molybdenum cofactor of the Aio enzyme (Muller et al. 2007). Such a genetic organization has also been observed in Thiomonas arsenitoxydans (Arsène-Ploetze et al. 2010; Bertin et al. 2012) and the presence of aio genes on a plasmid has been reported in Nitrobacter hamburgensis and Thermus thermophilus str. HB8 (Bertin et al. 2012). These observations suggest that aioBA genes may be acquired by horizontal gene transfer.

The adaptive response to arsenic has been recently shown as occurring in two steps (Cleiss-Arnold et al. 2010). First, bacterial cells express various genes involved in defence mechanisms, for example, oxidative stress and arsenic efflux. Next, several metabolic activities are induced, including arsenite oxidation which, in heterotrophic bacteria like H. arsenicoxydans, may be principally considered as a detoxification mechanism (Muller et al. 2007). In contrast, in bacteria that can grow autotrophically such as T. arsenitoxydans (Arsène-Ploetze et al. 2010) arsenite oxidation is part of a bioenergetic mechanism involved in energy generation. Despite some similarities, the genome organization of these two bacteria and their arsenic response, including biofilm formation, have been shown to differ markedly (Marchal et al. 2010, 2011).

In their natural environment, bacteria usually grow in biofilms, which are structured microbial communities embedded in extracellular polymeric substances (EPS) composed of sugars, proteins, and DNA (Hall-Stoodley et al. 2004; McDougald et al. 2012). Even though biofilm formation can be a problem in the field of human health, it allows bacteria to survive and thrive in highly toxic environments, including those characterized by high concentrations of heavy metals or metalloids such as arsenic (Guibaud et al. 2006; Muller et al. 2007). Unlike H. arsenicoxydans (Marchal et al. 2010), T. arsenitoxydans has been shown to induce biofilm formation in the presence of As(III) (Marchal et al. 2011). In addition, after biofilm development, the induction of cell motility has led to accelerated cell dispersion, an important process in the colonization of alternative ecological niches.

To gain a better understanding of the genetic determinants involved in the metabolism of arsenic, we have investigated the response to As(III) in Rhizobium sp. NT-26, a motile, chemolithoautotrophic arsenite oxidizer isolated from a gold mine in Australia (Santini et al. 2000). This strain belongs to the Rhizobiaceae family of the Alphaproteobacteria, which includes many species living in association with plants, such as plant mutualists of the Rhizobium and Ensifer (formerly Sinorhizobium) genera (Martens et al. 2007) and plant pathogens or plant growth-promoting rhizobacteria of the Agrobacterium genus (Hao et al. 2011). The Rhizobium sp. NT-26 genome was sequenced and annotated, and its physiology was investigated using differential transcriptomics and proteomics, and random mutagenesis. Remarkably, the synthesis of flagella was shown to be controlled by arsenite, suggesting a possible coordinate regulation between clusters located on two genetic elements. Indeed, proteins involved in As(III) oxidation were shown to be encoded by genes present on a megaplasmid, whereas flagellar genes are located on the chromosome.

Materials and Methods

Bacterial Strains, Plasmid, and Growth Conditions

Rhizobium sp. NT-26 and its mutant strains were cultivated at 28 °C in minimal salts medium (MSM) containing 0.04% yeast extract (Santini et al. 2000) and supplemented with As(III) and agar when required. Escherichia coli S17.1 λpir was cultivated at 28 °C in Luria–Bertani (LB) (MP Biomedicals) medium supplemented with 20 mg/l kanamycin (Sigma) for the maintenance of the pTGN/mini-Tn5 gfp-km plasmid (Tang et al. 1999).

Random Mutagenesis and Screening

Using the suicide vector pTGN carrying the mini-Tn5 transposon, random mutagenesis was performed to construct a mutant library and to identify genes involved either in arsenite oxidation or in motility. Mobilization of the plasmid was performed using E. coli S17.1 λpir carrying plasmid pTGN as the

donor and *Rhizobium* sp. NT-26 as the recipient. For conjugation, both strains in exponential phase, respectively, corresponding to an optical density (OD) of 0.6 and 0.135 at 600 nm, were superposed on LB plates at 28 °C for 24 h. As the *Rhizobium* sp. NT-26 strain used in this study is rifampicin resistant (Santini and vanden Hoven 2004), mutants were then selected on LB plates supplemented with 20 mg/l kanamycin and rifampicin.

Colonies from the library were screened for the loss of arsenite oxidation or the loss of motility. Briefly, mutants were individually inoculated into 96-well microtiter plates containing MSM with 0.04% yeast extract and 8 mM As(III) and incubated at 28 °C in 1.5% agar for 48 h or 0.3% agar for 24 h, respectively. The library was screened in the following two ways: 1) the silver nitrate method was used to detect arsenite oxidation (Lett et al. 2001; Muller et al. 2003) and 2) the diameter of the swarming ring was used to determine whether the cells were motile (Muller et al. 2007). Each phenotype was subsequently confirmed on Petri dishes in the corresponding medium. Mutants unable to oxidize arsenite were also tested for motility and vice versa.

To identify the disrupted gene in each mutant, the genomic region close to the mini-Tn*5* insertion site was amplified by inverse polymerase chain reaction (PCR). Total DNA was extracted with the Wizard Genomic DNA purification kit according to the manufacturer's instructions (Promega). One microgram of DNA was digested with 50 U of restriction enzymes that do not cut the transposon sequence (ClaI or PstI) in a 50 µl reaction volume at 37 °C for 2 h. After precipitation by ethanol and sodium acetate, digested DNA was ligated with 10 U of DNA ligase (Fermentas) in a volume of 20 µl overnight at 16 °C. PCR was carried out on 25 ng of this template in a 25 µl volume reaction with iProof DNA Polymerase (Bio-Rad) and Oend (ACTTGTGTATAAGAGTCAG) and Iend (AGATCTGATCAAGAGACAG) primers. The program used involved a denaturation step at 98 °C for 30 s, followed by 35 cycles of denaturation at 98 °C for 10 s, annealing at 52 °C for 30 s and elongation at 72 °C for 3 min, and a final elongation step at 72 °C for 10 min. Amplification products were checked on an agarose gel and sequenced with Oend by MilleGen (http://www.millegen.com/, last accessed April 30, 2013). The Blastn tool on the MaGe interface (Vallenet et al. 2006) was used to align the sequences with that of the *Rhizobium* sp. NT-26 genome allowing for identification of the disrupted gene. For each mutant, the precise insertion site and orientation of the mini-Tn*5* was determined by PCR, combining the Oend and Iend primers with new specific primers (supplementary table S1, Supplementary Material online) designed around each probable insertion site.

Biofilm Quantification

Biofilm formation by *Rhizobium* sp. NT-26 wild-type and mutant strains grown in the presence or absence of arsenite was measured by the crystal violet method. Cultures were grown in MSM medium containing 0.04% yeast extract supplemented with and without 8 mM As(III) and incubated at 28 °C overnight with shaking (120 rpm). The cultures were then diluted with fresh medium to an OD of 0.1 at 600 nm. Each strain was tested with six replicates of 200 µl in two flat-bottomed polystyrene 96-well microtiter plates (Nunc). Cultures were incubated at 28 °C for 24 h and 48 h without agitation. Biofilm formation was quantified using crystal violet, as previously described (Hommais et al. 2002). Briefly, after removing the culture medium, wells were gently rinsed three times with 0.1 M phosphate-buffered saline (PBS). To fix biofilms, plates were dried at 55 °C for 25 min, then 200 µl of 0.1% [w/v] crystal violet solution (Merck) was added to the wells and the plates were incubated at 30 °C for 30 min. Free crystal violet was removed and wells were washed three times with PBS. Plates were dried at room temperature and the biofilm was subsequently dissolved in 200 µl of 95% [v/v] ethanol over 30 min. Finally, the absorbance was read at 595 nm with a microplate reader (Synergy HT).

Pulsed-Field Gel Electrophoresis

Plasmid profiles were determined by a modified Eckhardt agarose gel electrophoresis technique, as described previously (Hynes and McGregor 1990). *Rhizobium* sp. NT-26 was grown in LB until an OD of 0.5 at 600 nm was reached, and 150 µl of culture were used per well. Electrophoresis was carried out at 4 °C, 5 V for 30 min and 85 V for 7 h on a 0.7% agarose gel containing 1% [w/v] sodium dodecyl sulfate (SDS) (Ramírez-Bahena et al. 2012). Plasmid size was estimated by comparison with those from *Agrobacterium tumefaciens* C58 (Wood et al. 2001).

Plant Trapping Tests

Nodulation experiments were performed under gnotobiotic conditions. Seeds of *Macroptilium atropurpureum*, *Vicia faba*, *Phaseolus vulgaris*, and *Pisum sativum* were surface sterilized for 2 min in 95% ethyl alcohol and then three times for 3 min in 1% sodium hypochlorite, each time washed with sterile water. Germination was carried out at 28 °C in dark conditions on glass plates covered with sterile filter paper moistened with sterile water. Pots with a capacity of 1.5 l were filled with sterile vermiculite, and 200 ml of nutrient sterile solution (Rigaud and Puppo 1975) was added per pot. Two seedlings were sown in each pot and plants were inoculated with a suspension of 10^5 CFU/ml 1 week after their transfer to hydroponic growth. *Rhizobium* sp. NT-26 was grown on YMB medium (Mannitol 0.7%, Yeast extract 0.2%, KH_2PO_4 0.02%, $MgSO_4$ 0.02%) and 1 ml of inoculum was applied to each seedling. Plants were regularly observed for nodule formation, and nodulation was quantified after inoculation as described in Gremaud and Harper (1989).

Genome Sequencing

The complete genome sequence of *Rhizobium* sp. NT-26 was obtained by combining Sanger and 454 sequencing methods. Sanger reads were obtained from a 10 kb insert library constructed after mechanical shearing of the genomic DNA and cloning of the generated inserts into the plasmid pCNS, as described previously (Muller et al. 2007). Plasmid DNA was purified and end-sequenced (26,888 reads) by dye-terminator chemistry with ABI3730 sequencers (Applied Biosystems) leading approximately to a 4× coverage. Reads were assembled by Newbler with around 20× coverage of 454 GS FLX reads (Roche) and validated via the Consed interface. Finishing steps were performed using primer walking of clones, PCR and in vitro transposition technology with the Template Generation System II Kit (Finnzyme), corresponding to 252, 32 and 8,404 additional reads, respectively. Approximately 70× coverage of 36 bp Illumina reads were mapped in the polishing phase, using SOAP (http://soap.genomics.org.cn/, last accessed April 30, 2013), as previously described (Aury et al. 2008).

Comparative Analysis of 24 *Rhizobiaceae* Genomes

The 23 genomes of *Rhizobiaceae* publicly available at the time of experiments (supplementary table S2, Supplementary Material online) were retrieved from ENA database (http://www.ebi.ac.uk/ena/, last accessed April 30, 2013). A homologous gene family database was built under the HOGENOM procedure (Penel et al. 2009) based on these 23 genomes and the one of *Rhizobium* sp. NT-26. Homologous protein sequences were aligned using MUSCLE (v.3.8.31, default parameters) (Edgar 2004) and then retro-translated with the pal2nal program (v.14) (Suyama et al. 2006). Nucleic acid alignments were restricted to conserved blocks with Gblocks (v.0.91b, minimum 50% of sequences in conserved and flank positions and all gaps allowed, codon mode) (Castresana 2000) and gene trees were computed from these alignments with PhyML (v.3.0, GTR + G8 + I model of evolution, best of SPR and NNI moves, SH-like branch supports) (Guindon and Gascuel 2003). All alignments and phylogenetic trees are shown in supplementary methods S1 and S2, Supplementary Material online. Replicon mapping and gene content comparison were done with custom Python scripts.

Species Phylogenies

The "core" set contained 822 gene families present in every 24 strains in only one copy. The "ribosomal" set contained 51 gene families whose products were annotated as "ribosomal protein" or related terms in at least one genome and were present in at least 22 strains. Full alignments of both family sets, and third codon-removed version of core family set were concatenated and used for species tree construction with RaxML (version 7.2.8-ALPHA, GTRCAT model with 50 categories, branch supports from 200 and 1,000 rapid bootstrap trees for "core" and "ribosomal" alignments, respectively)

(Stamatakis 2006) (species trees are stored in supplementary methods S3, Supplementary Material online).

Tree Pattern Matching

Phylogenetic trees of gene families were searched for particular phylogenetic patterns, that is, subtrees with specific arrangement of relative branching leaves representing taxa, with TPMS software (Bigot et al. 2012): "NT26outAgro", that is *Rhizobium* sp. NT-26 as a direct outgroup of *Agrobacterium* genus; "NT26inAgro", that is *Rhizobium* sp. NT-26 as an ingroup of *Agrobacterium* and sister group of *A. tumefaciens*. Both searches were made first without considering branch support and then matching only with >0.9 SH-like branch support at nodes of interest (supplementary methods S4, Supplementary Material online).

Aio Phylogenies

Homologs of AioA, AioB, AioR, AioS, and AioX were retrieved from the nr database at the NCBI (http://www.ncbi.nlm.nih.gov/, last accessed April 30, 2013) using the BlastP program (Altschul et al. 1997) with the protein sequences of *Rhizobium* sp. NT-26 as queries and default parameters except the "Max target sequences" parameter which was set to 1,000. For each Aio protein, the 500 homologs displaying the highest similarity with the sequence of *Rhizobium* sp. NT-26 were retrieved and aligned using MAFFT (version 6, default parameters) (Katoh and Toh 2008). The resulting alignments were trimmed using BMGE (default parameters) (Criscuolo and Gribaldo 2010). Preliminary phylogenies were inferred using the Neighbor-Joining method implemented in SeaView (Poisson evolutionary distance) (Gouy et al. 2010). The robustness of the resulting trees was estimated with the nonparametric bootstrap procedure implemented in SeaView (100 replicates of the original alignments). Based on the resulting trees, the closest relatives of *Rhizobium* sp. NT-26 sequences were identified and used for more detailed phylogenetic analyses. The corresponding sequences were realigned and the resulting alignments trimmed using the same procedure. Final phylogenetic analyses were performed using the maximum likelihood and Bayesian approaches implemented in PhyML (version 3) (Guindon et al. 2009) and MrBayes (version 3.2) (Ronquist et al. 2012), respectively. PhyML was run with the LG evolutionary model (Le and Gascuel 2008) and a gamma distribution with four categories of substitution rates (Γ4) and an estimated alpha parameter. The robustness of the maximum likelihood trees was estimated by the nonparametric procedure implemented in PhyML (100 replicates of the original alignments). MrBayes was run with a mixed substitution model and a Γ4 distribution. Four chains were run in parallel for 1,000,000 generations. The first 2,000 generations were discarded as "burnin." The remaining trees were sampled every 100 generations to build the consensus tree.

Total RNA Extraction, Microarrays, and Data Analysis

A custom 15 K microarray with a probe length of 60 mer was manufactured by Agilent Technologies following the protocol used for *H. arsenicoxydans* (Weiss et al. 2009). Total RNA was extracted from *Rhizobium* sp. NT-26 strain grown heterotrophically in MSM containing 0.04% yeast extract in the absence and presence of 5.3 mM As(III) until late log phase (OD at 600 nm of 0.115 and 0.152, respectively) as described previously (Santini et al. 2007). RNA quality was checked using an Agilent Bioanalyzer. Ten micrograms of total RNA was reverse transcribed using the Fairplay III Microarray labeling kit (Agilent Technologies) and cDNA were indirectly labeled using Cy3 or Cy5 Mono reactive dyes (GE Healthcare). Labeled cDNA quality and quantity were determined by spectroscopy at 260, 280, 550, and 650 nm. The labeled Cy3 and Cy5 target quantities were adjusted to 250 pmol, mixed together and concentrated with Microcon YM-30 (Millipore). Hybridization was performed for 17 h at 65 °C. Three distinct biological RNA samples as well as dye swap experiments were performed for each culture condition. Arrays were scanned as described previously (Weiss et al. 2009). Data were acquired by Genepix Pro 6.0 (Axon Instrument) and statistically analyzed as described previously (Koechler et al. 2010). Genes having a BH adjusted *P* value lower than 0.05 were considered as differentially expressed between the two conditions and were retained for further study. Microarray data were deposited in ArrayExpress (E-MEXP-3021).

Preparation of Proteins Extracts and 2D Gel Electrophoresis

Experiments were performed with four protein extracts from four replicates for each growth condition. Strain NT-26 was grown heterotrophically in MSM containing 0.04% yeast extract in the absence or presence of 5.3 mM As(III). Exponential phase cultures were harvested by centrifugation at $6,000 \times g$ for 10 min at 4 °C. Pellets were suspended in 400 µl of distilled water supplemented with 1 µl Benzonase Nuclease (Sigma) and 4 µl of Protease Inhibitor Mix (GE Healthcare). Cell suspensions were sonicated on ice with 10 pulses of 30 s at 28% of amplitude with 30 s intervals using a VC 750 sonicator (Bioblock Scientific). Cellular debris were removed by two centrifugations, the first at $6,000 \times g$ for 5 min and the second at $16,000 \times g$ for 90 min. Protein concentrations were measured using the Bradford method (Bradford 1976).

Differential accumulation of proteins was either monitored by Colloidal Brilliant Blue staining or DIGE (Marouga et al. 2005). For Colloidal Brilliant Blue staining experiments, 300 µg of protein extract were diluted to a final volume of 350 µl with rehydration buffer (8 M urea, 2% [w/v] CHAPS, 0.5% [v/v] IPG buffer pH 3-10, 40 mM DTT, and 0.01% [w/v] bromophenol blue). For DIGE experiments, 50 µg of protein was adjusted to pH 8.8 by adding 50 mM Tris–HCl final concentration, and either stained with 400 pmol of Cy3 or Cy5

(GE Healthcare). In addition, 25 µg of each 8 extracts (4 replicates for 2 conditions) were pooled and stained with 1,600 pmol of Cy2 to serve as an internal standard. For the staining, each CyDye DIGE fluor stock solution was diluted in high grade dimethylformamide to a final concentration of 400 pmol/µl. One microliter of the dilution was added to 50 µg of protein (Cy3 and Cy5) or 4 µl to 200 µg of the internal standard pool (Cy2) and kept in the dark and on ice for 30 min. The reaction was stopped by adding 1 µl of a 10 mM solution of lysine to 50 µg of protein (4 µl to 200 µg) and then 1 volume of 2× sample buffer (9 M urea, 3 M thiourea, 130 mM DTT, 4% [w/v] CHAPS, 2% [v/v] IPG buffer Pharmalyte 3-10) was added prior to incubation on ice for 10 min. One Cy3-labeled sample (condition 1) and one Cy5-labeled sample (condition 2) were mixed with one-fourth of the Cy2-labeled pool and rehydration buffer was added to reach a volume of 350 µl. Dye swap experiments were performed for each culture condition.

For protein separation, samples were first loaded onto an 18 cm pH 4–7 IPG strip. IEF was conducted using the Ettan IPGphor system (GE Healthcare), as previously described (Weiss et al. 2009). The strips were equilibrated in SDS equilibration buffer (30 mM Tris–HCl pH 8.8, 6 M urea, 34.5% [v/v] glycerol, 2% [w/v] SDS, 0.01% [w/v] bromophenol blue) supplemented with 1% [w/v] DTT for 15 min and then with 2.5% [w/v] iodoacetamide for 15 min. SDS polyacrylamide gel electrophoresis was subsequently performed using 11.5% SDS gels, using the Ettan DAlt*six* system (GE Healthcare) with the following steps: 1 h at 60 mA, 80 V, 4 W and 1 h at 240 mA, 500 V, 52 W. Gels were stained with Colloidal Brilliant Blue or digitized using a Typhoon Scanner (GE Healthcare).

Differential protein expression analysis was performed as previously described (Bryan et al. 2009; Weiss et al. 2009). Spots were selected and identified by MALDI-TOF and Nano LC-MS/MS, and data analysis were performed with Mascot (Matrix Science Ltd.) as described previously (Bryan et al. 2009) against a *Rhizobium* sp. NT-26 protein database. All identifications were incorporated into the "InPact" proteomic database developed previously (http://inpact.u-strasbg.fr/~db/, last accessed April 30, 2013) (Bertin et al. 2008).

Transmission Electron Microscopy

Rhizobium sp. NT-26 or the *aioR* mutant were grown in MSM containing 0.04% yeast extract in the presence or absence of 8 mM As(III) for 24 h. A drop of culture was deposited onto Formvar-coated nickel grids and after cell decantation, the liquid excess was removed. Uranyl acetate 2% was added to negatively stain bacteria and flagella and these samples were dried. Grids were observed with a Hitachi H-600 transmission electron microscope (TEM) at 75 kV and photographed with a Hamamatsu ORCA-HR camera using the AMT software (Advanced Microscopy Techniques).

Results and Discussion

General Genome Features

Chromosome, Plasmids, and Genomic Plasticity

The *Rhizobium* sp. NT-26 genome includes a single 4.2 Mbp chromosome and two plasmids. The circular chromosome consists of 4,239,731 bp with 4,380 coding sequences, including 4,303 coding DNA sequences and 59 RNA genes, and representing 90.28% of the whole genome (fig. 1). Among these coding sequences (CDS), 34.40% are of unknown function.

The mean G + C content of the chromosome is 61.97% but its distribution is not homogenous (fig. 1), and the *Rhizobium* sp. NT-26 chromosome exhibits 65 regions of genomic plasticity (RGP, supplementary table S3, Supplementary Material online) (Vallenet et al. 2009) in comparison with that of *A. tumefaciens* 5A. The G + C content of these regions, their size (5–207 kb) and the codon adaptation index lower than the average are characteristic of genomic islands (GEI) (Juhas et al. 2009). Moreover, transposable elements and tRNA encoding genes are present in several of these regions, which further support the lateral transfer of these potential genomic islands (Daubin et al. 2003). Such genetic events are

known to promote bacterial adaptation under environmental stresses by the acquisition of various capacities through horizontal gene transfer, an important mechanism of microbial genome evolution (Juhas et al. 2009). In agreement with this, more than 15 loci coding for metabolic functions that may improve the fitness of the strain to its environment were found among the 65 RGP identified in the genome of *Rhizobium* sp. NT-26. These include amino acids and carbon sources transport, inorganic carbon fixation, nitrogen metabolism, and sulfur oxidation (supplementary table S3, Supplementary Material online).

The genomes of bacteria in the *Agrobacterium* and *Rhizobium* genera are known to include several extrachromosomal replicons, which encode various functions required for the adaptation to specific niches (López-Guerrero et al. 2012). The *Rhizobium* sp. NT-26 genome comprises two plasmids, including a megaplasmid of 322,264 bp containing 367 coding sequences (CDS) (fig. 1). The presence and the size of the megaplasmid were confirmed experimentally by a modified Eckhardt gel electrophoresis method (supplementary fig. S1, Supplementary Material online). The second plasmid is 15,430 bp and more than half of its CDS encode proteins with unknown functions.
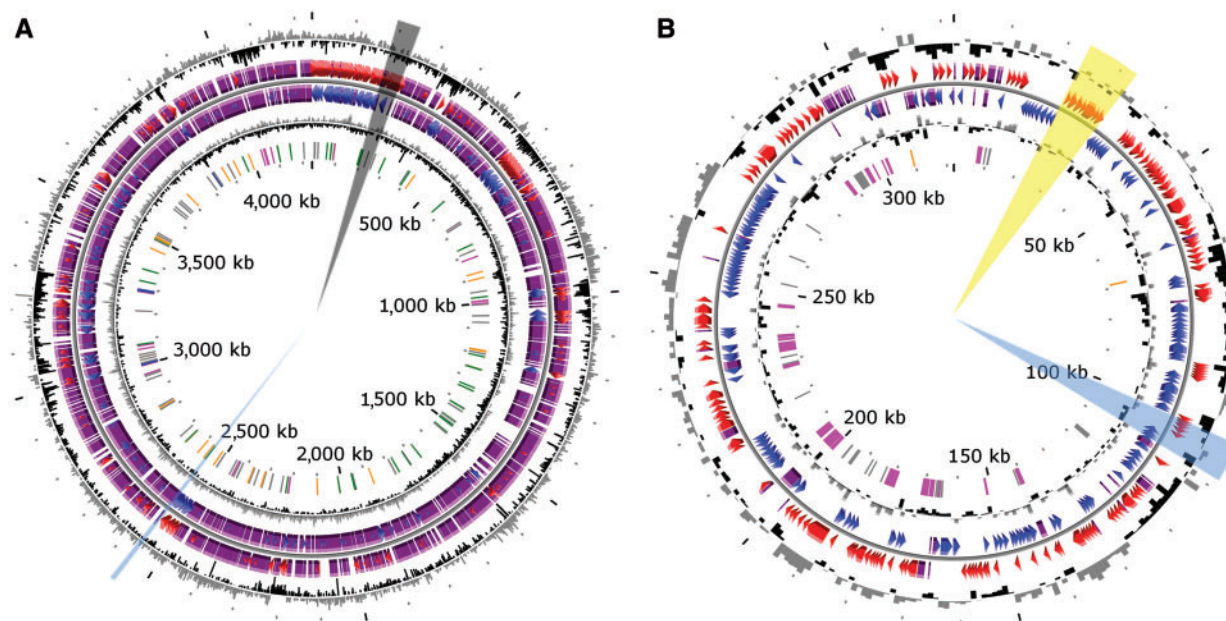

FIG. 1.—Circular representation of the *Rhizobium* sp. NT-26 genome. The chromosomal (*A*) and plasmidic (*B*) characteristics are 4,239-Mb long, 61.97% GC, 9 16S-23S-5S rRNA, 50 tRNA, and 4,294 CDSs; and 322-kb long, 60.19% GC, 0 16S-23S-5S rRNA, 0 tRNA, and 367 CDSs, respectively. From outside, circles display 1) the GC percent deviation in a 1,000 bp window (GC window − mean GC); 2) and 3) predicted CDSs transcribed in the clockwise and counterclockwise direction, respectively; red and blue colors correspond to validated annotations, orange to automatic annotation and purple to primary automatic annotation; 4) GC skew (G + C/G − C) in a 1,000 bp window; 5) rRNA are shown in blue, tRNA in green, miscRNA in orange, transposable elements in pink, and pseudogenes in gray. The regions with the genes coding for proteins involved in motility, reduction of arsenate or oxidation of arsenite are highlighted in black, blue, or yellow, respectively. The figure does not represent the p2 plasmid and the scale between the two genetic determinants is not respected (https://www.genoscope.cns.fr/agc/microscope/home/index.php, last accessed April 30, 2013).

The large plasmid harbors four different replication systems, in particular three *repABC* operons. The first one is duplicated. These two *repABC* operons are related to *repABC* of *Dinoroseobacter* (>90% identity) of the *Rhodobacteraceae,* a family of the *Rhodobacterales*. The third *repABC* operon is related to *repABC* of *Rhizobiales*. The fourth replication system is composed of a ParB/RepC replication system homolog of *A. tumefaciens* NCPPB925 plasmid origin of replication. Such a redundancy is not rare in *Rhizobiales*. For example, two replicons in *R. etli* CFN42, one in *R. leguminosarum* 3841 and one in *Ruegeria* sp. PR1b contain two *repABC* operons (Zhong et al. 2003; González et al. 2006; Young et al. 2006).

The smaller plasmid replication system is different from the canonical *repABC* replication system. It is constructed as the replication system described in pTAR of *A. vitis* (Gallie and Kado 1988), that is, the origin region carries a *repA*-like gene, a *parA* gene and a putative regulator locus coding for a putative segregation protein. Besides these replication transfer genes, the 15 kb plasmid harbors a toxin antitoxin system, which may explain its maintenance in *Rhizobium* sp. NT-26.

Plasmidic Adaptive Traits

In symbiotic bacteria, plasmids are known to play a role in their interaction with plants (López-Guerrero et al. 2012). In addition to multiple transposases and insertion sequences, the megaplasmid identified in *Rhizobium* sp. NT-26 encodes a putative type IV secretion system known to be involved in conjugal DNA transfer, including between bacteria and plants. Indeed, two complete *tra* clusters were found on the 322 kb plasmid: the first one is related to the type IV secretion system found in the *Rhizobium/Agrobacterium* genus, whereas the second one is related to the type IV secretion system of marine bacteria members of the *Rhodobacteraceae* family, that is, *Oceanibulbus indolifex* or *Ruegeria* sp. PR1b plasmid pSD25. However, canonical *nodABC* genes coding for proteins NodA (acetyl transferase), NodC (oligomerization of *N*-acetyl-glucosamine), and NodB (chitooligosaccharide deacatylase) that are required for the synthesis of the core structure of lipo-chitooligosaccharide (i.e., Nod factor) (Dénarié et al. 1996) were not identified in the genome of *Rhizobium* sp. NT-26. CDS displaying some similarities with other *nod* genes, that is, encoding enzymes that control specific substitutions on the chitooligosaccharide backbone, or the *fix* operon are present (supplementary table S4, Supplementary Material online), but these genes are also well conserved in nonsymbiotic prokaryotes. Nevertheless, it has been demonstrated that the nodulation of some *Fabaceae* by rhizobia occurs in the absence of the *nodABC* genes and lipo-chitooligosaccharidic Nod factors (Giraud et al. 2007). This indicates that other signaling strategies can trigger nodule organogenesis in some legumes. Nodulation assays on various *Fabaceae* plants were therefore performed as previously described (Gremaud and Harper 1989), but no nodules were

observed at 3 weeks after inoculation or later at 4 weeks (data not shown).

Despite a lack of plant nodulation, root inoculation by *Rhizobium* sp. NT-26 suggested a potential phytobeneficial effect (fig. 2). Direct plant-growth promotion can be derived from phosphorus solubilization (Richardson et al. 2009), production of plant growth regulators (phytohormones) such as auxins, gibberellins, and cytokinins (Spaepen et al. 2009), NO production and/or by supplying biologically fixed nitrogen (Creus et al. 2005). Increasing the bioavailability of phosphate as micronutrient is mediated by bacterial phosphatase activity, and a phosphatase homolog, that is, NT26v4_0651, is present in the *Rhizobium* sp. NT-26 genome. Moreover, two main classes of dissimilatory nitrite reductase (Nir) involved in NO production exist among denitrifying bacteria: the heme-cyto-chrome cd_1 type encoded by *nirS* genes and the copper-containing type encoded by *nirK* genes (Zumft 1997). A *nirK* homolog but no *nirS* homolog was identified in the *Rhizobium* sp. NT-26 genome. Finally, no other homolog of classical phytobeneficial functions was identified when analyzing the genome, for example, phytohormone synthesis such as auxin by *ipdC/ppdC* or aceton-2,3-butanediol by *budABC*, or nitrogen fixation by nitrogenase *nifHDK*.

Indirect plant growth-promoting mechanisms used by plant-growth-promoting rhizobacteria (PGPR) include induced systemic resistance, antibiotic protection against pathogens, reduction of iron availability in the rhizosphere by

Fig. 2.—Phytobeneficial effect of *Rhizobium* sp. NT-26 on *Phaseolus vulgaris*. Erlenmeyer flasks of *P. vulgaris* were inoculated with *Rhizobium* sp. NT-26 on the left, and with water on the right.

sequestration with siderophores, synthesis of fungal cell wall-lysing or lytic enzymes, and competition for nutrients and colonization sites with pathogens (Dobbelaere and Okon 2007). *Rhizobium* sp. NT-26 contains loci coding for polyketide synthases (NT26v4_3331, NT26v4_3332, and NT26v4_3333), which are involved in nonribosomal synthesis of antibiotics, or coding for proteins involved in siderophore transport (NT26v4_2008, NT26v4_4195, and NT26v4_4199). Taken together, these observations suggest that *Rhizobium* sp. NT-26 does not exert any direct interaction with plants but it may have an indirect role in plant growth and protection by its metabolic activities in the rhizosphere.

Unlike *H. arsenicoxydans* (Muller et al. 2007) and *T. arsenitoxydans* (Arsène-Ploetze et al. 2010), which metabolize and provide resistance to arsenic using proteins encoded by chromosomally borne genes, proteins involved in arsenic resistance in *Rhizobium* sp. NT-26 are encoded by *ars* genes present on both the chromosome and the megaplasmid. The *aio* genes involved in arsenite oxidation are present only on the megaplasmid (fig. 1*B*), as shown in *The. thermophilus* str. HB8. The *Rhizobium* sp. NT-26 *aio* cluster also contains genes coding for phosphate transport and molybdenum cofactor biosynthesis, as previously observed in other arsenite-oxidizing bacteria (Arsène-Ploetze et al. 2010; Bertin et al. 2011). In addition, like the metallo-resistant strain *Cupriavidus metallidurans* (Janssen et al. 2010), the *Rhizobium* sp. NT-26 megaplasmid contains numerous genes involved in resistance to heavy metals such as chromium, cadmium, and mercury. These observations suggest a loss of most plasmid-encoded functions known to be involved in bacteria–plant interactions and an acquisition of multiple genes allowing the organism to grow in its natural habitat, a goldmine known to contain toxic metals and metalloids.

The gene cluster coding for arsenite oxidase contains 5 *aio* genes in *Rhizobium* sp. NT-26. The survey of the nr database revealed the existence of numerous homologs of AioA, AioB, AioR, AioS, and AioX. Preliminary phylogenetic analyses of AioA homologs showed that the sequence from *Rhizobium* sp. NT-26 belongs to a well-supported clade of proteobacterial sequences corresponding to the groups I and II, which were recently described (Heinrich-Salmeron et al. 2011). Subsequent phylogenetic analyses revealed that the *Rhizobium* sp. NT-26 AioA branched among alphaproteobacterial sequences (group I), within a strongly supported clade composed of sequences from various *Agrobacterium* species and *Sinorhizobium* sp. M14 (Rhizobiaceae), from *Ochrobacterium tritici* (Brucellaceae), and uncultured organisms (bootstrap value [BV] = 98% and posterior probability [PP] = 1.00, supplementary fig. S2*A*, Supplementary Material online). Phylogenetic analyses of other Aio proteins showed similar branching patterns (supplementary fig. S2*B–E*, Supplementary Material online). This suggests that the five *aio* genes have co-evolved, which is not entirely surprising

given that they are functionally related and clustered together when present in a genome.

A careful examination of the taxonomic distribution within the subgroups (supplementary fig. S2, Supplementary Material online) revealed that only 2 *Rhizobium/Agrobacterium* complete genomes contain the *aio* genes although nearly 30 genome sequences are available at NCBI. In addition, the relationships among the sequences were not always in agreement within the phylogeny of species, for example, the grouping of a member of *Brucellaceae* within *Rhizobiaceae*. This strongly suggests that horizontal gene transfers may have played a role in the spread of *aio* genes among these species. The alternative hypothesis, that is the presence of *aio* genes in the common ancestor of the *Rhizobium/Agrobacterium* group followed by multiple independent gene losses during the diversification of this lineage, appears less likely and does not explain the discrepancies among the Aio phylogenies and the taxonomy. On the contrary, these inconsistencies may be easily explained by the initial acquisition of the *aio* genes by one member of the *Rhizobium/Agrobacterium* group followed by a few horizontal gene transfers to related species or strains. Such transfers may have been favored by the colocation of *aio* genes on genomes and their location on plasmids in a few strains (e.g., pSinA in *Sinorhizobium* sp. M14 and pAt5A for *A. tumefaciens* 5A).

Taxonomic Relationship of *Rhizobium* sp. NT-26 with Other *Rhizobiaceae*

Rhizobium sp. NT-26 strain has been previously assigned to the *Rhizobium* genus on the basis of 16S RNA sequence (Santini et al. 2000), but its phylogenetic relationship with other *Rhizobiaceae* remains quite unclear. Therefore, the sequence of the *Rhizobium* sp. NT-26 chromosome has been compared with the sequences present in the "Prokaryotic Genome DataBase" (PkGDB) (Vallenet et al. 2006) and RefSeq (NCBI Reference Sequences) data banks. The highest synteny conservation was observed with the *A. tumefaciens* C58 circular chromosome, which is 67.85% of the CDS in this genome share synteny with the chromosome of *Rhizobium* sp. NT-26 and the average size of the syntons is 8.4 CDS. This gene order conservation is higher than that observed with *Rhizobium* spp. strains (6.9–7.4), suggesting a closer evolutionary relationship of strain *Rhizobium* sp. NT-26 with the *Agrobacterium* lineage. To determine more precisely the taxonomic position of *Rhizobium* sp. NT-26 among *Rhizobiaceae*, we compared its genome with a set of 23 other sequenced genomes of this family in a phylogenetic framework. We computed maximum-likelihood (ML) trees based on the concatenated alignments of sequences of either all-homologous genes that are common to and unique in all strains (822 "core" genes) or genes of ribosomal proteins (51 "ribosomal" genes). Intriguingly, both data sets yielded phylogenies that agree on all major splits in the taxon, but not on the position
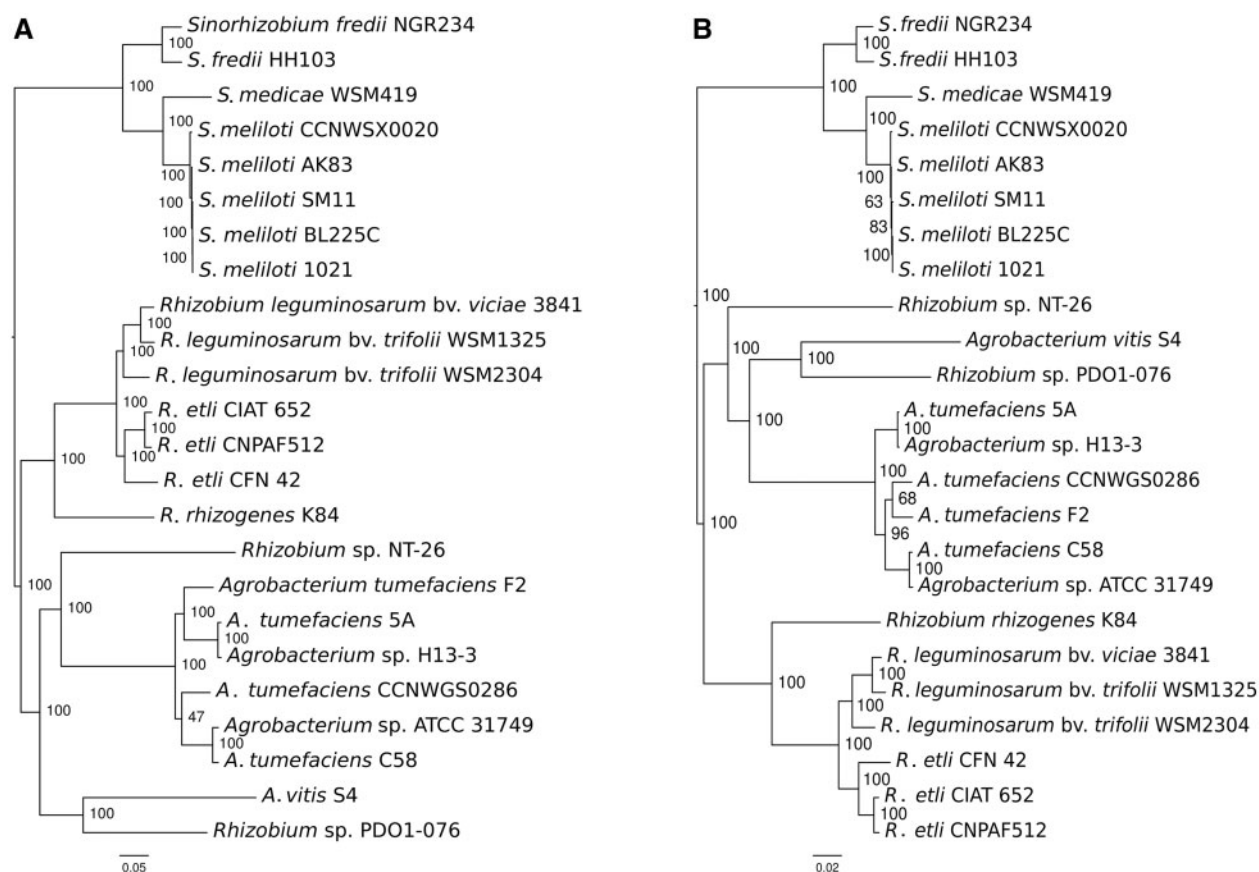
FIG. 3.—Phylogeny of *Rhizobium* sp. NT-26 among *Rhizobiaceae*. ML phylogenies of 24 *Rhizobiaceae* including strain NT-26 were built from concatenated alignments of (*A*) 822 core genes and (*B*) 51 ribosomal genes. Branch supports are percentage of the 200 and 1,000 bootstrap trees having the bipartition, respectively.

of *Rhizobium* sp. NT-26. According to core genes, this strain branched as an "in-group" of the *Agrobacterium* subgroup, being the brother clade of *A. tumefaciens* after the split with *A. vitis* (fig. 3*A*). Instead, according to ribosomal genes, strain NT-26 branched as an "out-group" of the *Agrobacterium* clade that encompasses *A. vitis* and *A. tumefaciens* (fig. 3*B*). In both cases, the conflicting bipartitions are well supported, and removing third codon positions in the alignment of core genes, because of the possible saturation of the substitution signal in non-housekeeping genes, did not change the observed pattern (supplementary methods S3, Supplementary Material online). This suggests that among the core gene set, which include the majority of the ribosomal gene set, different genes have different histories, causing the average history (core phylogeny) to be different from that of a subset (ribosomal phylogeny). This may have been caused by horizontal gene transfer to and from *A. tumefaciens*, *A. vitis*, *Rhizobium*, or other more phylogenetically distant taxon that would blur the signal for vertical inheritance.

We therefore computed individual phylogenies for all homologous families to determine what scenario each gene

supported. On a set of 2,878 homologous gene family trees containing 3,537 *Rhizobium* sp. NT-26 genes, we searched for subtrees displaying the unambiguous patterns of either *Rhizobium* sp. NT-26 as a direct out-group of the *Agrobacterium* clade ("NT26outAgro") or as an in-group of the *Agrobacterium* clade and a brother group of *A. tumefaciens* ("NT26inAgro"). "NT26inAgro" was prevalent with 338 genes (268 considering only high branch support) versus 255 (146) for "NT26outAgro," and even though the amount of genes displaying such unambiguous patterns was relatively low, "NT26inAgro" was significantly more frequent (χ^2 test, P value $< 10^{-3}$). The location of those genes along the chromosome of *Rhizobium* sp. NT-26 showed no grouping with a particular pattern that could support a large-scale transfer event (Mann–Whitney–Wilcoxon test, P value >0.9; supplementary fig. S3, Supplementary Material online). The homogeneous dispersal of phylogenetic signatures rather suggests that numerous small-scale transfer events occurred, as observed in the case of frequent homologous recombination with partners of different taxa (Didelot et al. 2010). Alternatively, our observations may be the consequence of a

poor resolution of phylogenies. This may be due to the frequent artifacts in the phylogenetic reconstruction of the relationship of strain NT-26 to *Agrobacterium*, such as those caused by the long branch leading to *Rhizobium* sp. NT-26. In the future, more phylogenetic information might be provided by sampling strains branching at the base of the *Rhizobium/Agrobacterium* group.

Most of *Rhizobiaceae* contain a secondary chromosome or megaplasmids, generally referred to as chromids (Harrison et al. 2010), that are members of a same family of large replicons derived from a plasmid (Slater et al. 2009). Although *Rhizobium* sp. NT-26 genome contains a megaplasmid with chromid characteristics (Harrison et al. 2010), this megaplasmid show very limited homology with chromids of this family (supplementary table S5, Supplementary Material online). The absence of a typical *Rhizobiaceae* secondary replicon makes the genome structure of *Rhizobium* sp. NT-26 unusual when compared with other members of the family. Comparison of the homologous gene location in *Rhizobium* sp. NT-26 and related organisms may help with the understanding of its evolution history. With this aim, the closest homolog of each of its genes present in several strains of *Rhizobium* and *Agrobacterium* were mapped along the *Rhizobium* sp. NT-26 chromosome (supplementary fig. S4, Supplementary Material online). It appeared that the vast majority of strain NT-26 chromosomal genes map to the principal chromosome in *Rhizobium* and *A. vitis*, suggesting that the *Rhizobium* sp. NT-26 lineage has completely lost the secondary chromosome of the *Rhizobium/Agrobacterium* ancestor. The history of intragenomic translocations have been documented in this taxon (Slater et al. 2009) and locating *Rhizobium* sp. NT-26 genes whose homologs have migrated at a specific divergence time would help to date the age of the divergence of the *Rhizobium* sp. NT-26 lineage. In this respect, its chromosome possesses a large chromosomal fragment (spanning from 2.55 to 3.40 Mb), which is specifically present on the secondary (linear) chromosome in *A. tumefaciens* (supplementary fig. 3, Supplementary Material online), further supporting a divergence of the *Rhizobium* sp. NT-26 lineage predating the *A. tumefaciens* speciation and synapomorphic translocation events. Similarly, strain NT-26 appears to have conserved the majority of the genes that are specifically borne by the secondary chromosome of *R. rhizogenes* (119 homologs in *Rhizobium* sp. NT-26 over 129 specific translocated genes). If strain NT-26 belonged to the *Rhizobium* lineage, the majority of these genes would probably have been lost with this whole chromid, although we cannot rule out potential translocations of those genes back to the main chromosome along with the chromid loss. Taken together, and even though our current data do not allow a more accurate classification, our observations support the inclusion of *Rhizobium* sp. NT-26 in the *Agrobacterium* subgroup. Nevertheless, according to the current nomenclature (Young

et al. 2001), *Rhizobium* is still a valid genus name for strain NT-26.

Finally, although chromosomes are mainly dedicated to housekeeping functions, chromids carry genes involved in specific ecological functions, that is, legume symbiosis enabled by symbiotic plasmids in *Rhizobium* and *Sinorhizobium* (Harrison et al. 2010) and plant-related functions in *A. tumefaciens* C58 (Lassalle et al. 2011). All these functions relate to the interactions inside the rhizosphere and soil that represent the canonical habitat of *Rhizobiaceae*. The loss by *Rhizobium* sp. NT-26 of this large replicon housing rhizosphere-associated functions may be related to the drastic shift in environment the lineage has experienced. Indeed (discussed earlier), this loss coincides with the gain of genes enabling resistance to heavy metals, and arsenic and sulfur metabolisms, both traits with a potentially great adaptive value in sustaining life on an arsenopyrite (FeAsS)-containing rock.

Functional Approaches to Investigate Arsenic Metabolism and Resistance

Proteomic and Transcriptomic Profiling

Genomic tools have been used to study the bacterial response to arsenic mainly in arsenite-oxidizing *Betaproteobacteria* such as *H. arsenicoxydans*, a chemoorganotroph (Carapito et al. 2006; Muller et al. 2007; Weiss et al. 2009), and *T. arsenitoxydans*, a chemolithoautotroph (Bryan et al. 2009; Arsène-Ploetze et al. 2010). Arsenic metabolism was investigated in the chemolithoautotrophic *Alphaprotebacterium Rhizobium* sp. NT-26 by two complementary approaches: protein and RNA profiling using 2D gel electrophoresis and DNA microarrays, respectively. The comparisons of expression were done on proteins and RNA isolated from strain NT-26 grown heterotrophically with and without arsenite. The main results are summarized in table 1 and a complete list of the data is presented in supplementary table S6, Supplementary Material online.

The 2D gel proteomic profile of *Rhizobium* sp. NT-26 was quite similar to those previously obtained for *H. arsenicoxydans* (Carapito et al. 2006) and *T. arsenitoxydans* (Bryan et al. 2009), which are also neutrophilic bacteria. Sixty-three spots showed a significant difference in their accumulation pattern in strain NT-26 grown with and without As(III). Their analysis by mass spectrometry led to the identification of 141 proteins (supplementary table S6a, Supplementary Material online), including arsenite oxidase, which was identified for the first time on 2D gels. Like membrane proteins, such periplasmic proteins are often eliminated with cell debris before their solubilization during sample preparation. Proteins up- or downregulated with a fold-change ranging from +39.6 to −5.8 when *Rhizobium* sp. NT-26 was grown in the presence of As(III) had a molecular mass ranging from 15 to 109 kDa and a pI value from 4.2 to 7.9. Among them, 24% were involved in cell envelope and cellular processes, 12% in

Table 1

Major Arsenic-Regulated Functional Categories Identified in Transcriptomics and Proteomics Experiments

Functional Category	MaGe ID	Gene	Function	FC	
				RNA[a]	Protein[a]
Oxidative stress	NT26v4_0103	rpoN	RNA polymerase σ^{54} factor	1.32	
	NT26v4_0389	katA	Catalase A	1.37	
	NT26v4_0773	ohr	Organic hyperoxide resistance	1.41	
	NT26v4_0799	sodB	Superoxide dismutase		3
Carbon metabolism	NT26v4_0674	cbbF	Fructose-1.6-bisphosphatase	1.3	
	NT26v4_0670	cbbL	RuBisCo large subunit	1.37	
	NT26v4_2684	cbbT	Transketolase		3.4
	NT26v4_0667	cbbE	Ribulose-phosphate 3-epimerase	1.35	
Nitrogen metabolism	NT26v4_3645	norQ	Putative NorD protein	1.52	
	NT26v4_3643	norC	Nitric oxide reductase subunit C	1.42	
	NT26v4_3641	norE	Involved in nitric oxide reduction	1.60	
	NT26v4_3654	nirV	Involved in nitrite reduction	1.51	
	NT26v4_3653	nirK	Cu-containing nitrite reductase		39.6
Arsenic metabolism	NT26v4_p10030	aioA	Arsenite oxidase large subunit	3.89	10
	NT26v4_p10029	aioB	Arsenite oxidase small subunit	4.27	
	NT26v4_p10118	arsC1b	Arsenate reductase ArsC		22
	NT26v4_p10122	arsH1	Arsenical resistance protein		2.9
Sulfur metabolism	NT26v4_2623	soxG	Sulfur oxidation protein	−1.37	
	NT26v4_2619	soxV	Sulfur oxidation protein	−1.39	
	NT26v4_2618	soxW	Thioredoxin	−1.52	
	NT26v4_2617	soxX	Sulfur oxidizing protein	−1.68	
	NT26v4_2616	soxY	Sulfur oxidation protein	−1.45	
	NT26v4_2615	soxZ	Sulfur oxidation protein	−1.51	
	NT26v4_2882	cysT	Sulfate/thiosulfate transport protein	−1.72	
Phosphate metabolism	NT26v4_1226	phoE1	Phosphonate ABC transporter	1.45	
	NT26v4_0079	phoR	Phosphate regulon kinase	1.32	
	NT26v4_p10016	phoE2	Phosphonate ABC transporter subunit	1.61	
	NT26v4_p10017	phoT2	Phosphonate ABC transporter subunit	1.42	
	NT26v4_p10024	pstS2	High-affinity phosphate transporter		3.7
Motility/biofilm	NT26v4_0204	fliF	Flagellar M-ring protein	1.44	
	NT26v4_0227	flaA	Flagellin A		7.2
	NT26v4_0228	fla	Flagellin		9.7
	NT26v4_0655	qseB	Quorum sensing regulator QseB	1.39	
	NT26v4_2748	noeJ	Mannose-1-P guanylyltransferase	1.41	
	NT26v4_1615	kdsA	KDO 8-P synthase	1.40	
Plant/bacteria interactions	NT26v4_1705	cgmA	Beta-1.2-glucan modification protein	1.7	
	NT26v4_p10302	avhB10	Type IV system transglycosylase	1.41	

NOTE.—Induced and repressed functions are shown in blue and black, respectively. No value is indicated in the FC column if the gene is not statistically differentially expressed in transcriptomics or if the protein has not been identified in proteomics. Complete data are presented in supplementary table S6, Supplementary Material online.
[a]Fold-change observed in transcriptomics and proteomics data, respectively.

transport and binding proteins, 11% in information and regulation pathways, 42% in metabolism, 1% in transcription, and 10% were of unknown function.

The second approach used whole genome microarrays to perform a differential expression profiling experiment. Under As(III) stress, the transcript level of 199 genes, that is 4.5% of the whole genome, showed an increase of up to more than four times with a P value ≤ 0.05. At the same time, the expression of 416 genes, that is 9.5% of the whole genome,

decreased by up to more than three times (supplementary table S6c, Supplementary Material online).

General Response to Arsenic Stress

Several proteins involved in arsenic resistance were shown to be accumulated on 2D gels when the organism was grown in the presence of As(III), for example, an ArsH1 NADPH-dependent FMN reductase and an ArsC1 arsenate

reductase (table 1) with fold changes of 2.9 and 22, respectively. These two proteins are encoded by an *ars* operon located on the megaplasmid, which also contains genes coding for an ArsB efflux pump and an ArsR regulator. Moreover, a second operon located on the chromosome contains an *arsA* gene coding for an ATPase associated with an ArsB arsenite efflux pump. ArsA enables the strain to increase arsenic resistance by ATP-dependent extrusion of the metalloid out of the cell (Branco et al. 2008).

Microarray experiments showed that genes encoding the two arsenite oxidase subunits, that is, the small subunit, AioB, which contains the Rieske 2Fe-2S cluster and the catalytic subunit, AioA, which contains a molybdopterin guanine dinucleotide at the active site and a 3Fe–4S cluster (Santini and vanden Hoven 2004), were about 4-fold induced in the presence of arsenite (table 1). In contrast, the expression of two genes located downstream of the *aioBA* operon, that is, *cytC* encoding the periplasmic cytochrome c_{552}, which can serve as an electron acceptor to the arsenite oxidase (Santini et al. 2007) and *moeA1* encoding a molybdenum cofactor biosynthesis gene, was not significantly affected under arsenite stress (supplementary table S6c, Supplementary Material online). These observations are further supported by proteomic experiments showing that, among these proteins, AioA was found to be preferentially accumulated in the presence of As(III). All these results are consistent with previous data (Santini et al. 2007), which suggests that the expression of *aioBA* genes is induced by arsenite while genes located downstream are constitutively expressed even though they may have a role in arsenic metabolism.

Located upstream of *aioBA* are two regulatory genes, *aioS* and *aioR*, which encode a sensor histidine kinase and a response regulator, respectively (Sardiwal et al. 2010). Both proteins have been shown to be required for the transcriptional regulation of the *aioBA* genes (Koechler et al. 2010; Sardiwal et al. 2010). Moreover, it has been demonstrated that the expression of the *aioBA* genes requires the RpoN alternative sigma factor (σ^{54}) in *H. arsenicoxydans* (Koechler et al. 2010). Similarly, a role for RpoN in arsenite oxidation has been recently highlighted in *A. tumefaciens* 5A (Kang et al. 2012). In this respect, a putative σ^{54}-dependent promoter region has been detected upstream of the *aioB* gene in *Rhizobium* sp. NT-26 (Santini et al. 2007), suggesting that it is also involved in the expression of the *aioBA* operon in strain NT-26 (Sardiwal et al. 2010). This hypothesis is supported by our transcriptomic data, which revealed an induced expression of *rpoN* in *Rhizobium* sp. NT-26 when it was grown in the presence of As(III) (table 1), in contrast to the constitutive expression recently observed in *A. tumefaciens* 5A (Kang et al. 2012). Similarly, microarray and 2D-gel data showed a 2-fold increase in the expression of genes coding for general chaperones, that is, DnaK and GroEL, in the presence of arsenite (supplementary table S6a and c, Supplementary Material online), which is in agreement with the role played by proteins of the

heat-shock family in As(III) oxidation in *H. arsenicoxydans* (Koechler et al. 2010).

Rhizobium sp. NT-26 also tolerates arsenate concentration greater than 0.5 M (Clarke A. and Santini J.M., unpublished data), suggesting the existence of an alternative mode of resistance. The first one is an Ars-type arsenic resistance system, components of which were found to be upregulated when the strain was grown with arsenite (discussed earlier) and the second is the presence of a specific phosphate transport system which is thought to limit arsenate entry into the cell (Weiss et al. 2009). Indeed, in *Rhizobium* sp. NT-26, the arsenic genomic island contains a *pst* operon in the vicinity of the *aio* operon. The *pst* operon encodes proteins implicated in the specific transport of phosphate into the cell to maintain a sufficient level of this ion despite the presence of arsenate, a structural analog of phosphate (Muller et al. 2007; Cleiss-Arnold et al. 2010). PstS2, a periplasmic protein involved in phosphate transport and encoded by this operon, had a 3.7-fold increase in expression when strain NT-26 was grown in the presence of As(III) (table 1). The *pst* operon is regulated by *phoR*, which encodes a membrane-associated protein kinase that phosphorylates PhoB in response to environmental signals. Indeed, microarray data showed that the expression of *phoR* was also upregulated in the presence of As(III) (table 1). Moreover, the PhoR protein may be involved in biofilm formation as *phoB* overexpression has been shown to increase biofilm formation in *A. tumefaciens* (Danhorn et al. 2004). This is supported by the presence in the vicinity of the *pho* chromosomal operon of a cluster of genes involved in EPS biosynthesis (NT26v4_1233–NT26v4_1263).

Arsenic is known to induce oxidative stress by generating free radicals (Bernstam and Nriagu 2000). An induction of genes involved in the resistance to such a stress has been previously observed in *Pseudomonas aeruginosa* and in *H. arsenicoxydans* under arsenite exposure (Parvatiyar et al. 2005; Weiss et al. 2009; Cleiss-Arnold et al. 2010). In *Rhizobium* sp. NT-26, an increase in *katA* mRNA, which encodes a catalase involved in the protection against oxidative stress by scavenging endogenously produced H_2O_2, was observed in microarray experiments (table 1). Similarly, the expression of *ohr*, which promotes bacterial resistance to hydroperoxide, was also up-regulated in *Rhizobium* NT-26 (table 1). Finally, results of the proteomic experiments showed a 3-fold increase in the SodB superoxide dismutase accumulation when strain NT-26 was grown in the presence of As(III). These observations further support the strong link, which exists in bacteria between arsenic response and protection against oxidative stress (Bertin et al. 2012).

Carbon, Nitrogen, and Energy Metabolism

Rhizobium sp. NT-26 is able to use various carbon or electron sources for growth. Indeed, multiple carbohydrates such as acetate, succinate, fumarate, lactate, glucose, fructose,

xylose, and galactose are potential carbon sources for this bacterium (Santini et al. 2000). Alternatively, *Rhizobium* sp. NT-26 is able to grow chemolithoautotrophically in the presence of bicarbonate as a carbon source, oxygen as an electron acceptor and arsenite as an electron donor (Santini et al. 2000). Transcriptomics and proteomics experiments revealed that several genes and proteins involved in the fixation of CO_2 via the Calvin cycle were upregulated with a fold change ranging from 1.3 to 3.4 when strain NT-26 was grown in the presence of As(III) (table 1). This is in agreement with the proteomics results obtained in *T. arsenivorans,* where an accumulation of the ribulose-1,5-biphosphate carboxylase/oxygenase large subunit and of the fructose-1,6-biphosphate has been observed when the organism was grown in the presence of As(III) (Bryan et al. 2009). Both strains may thus improve their capacity to fix CO_2 when arsenite is present.

In addition, our microarrays data showed that the expression of *nirV* encoding a protein involved in nitrite reduction was induced. Moreover, 2D-gel data showed that NirK, which also participates in the reduction of nitrite to nitric oxide, was 39.6 times more accumulated when strain NT-26 was grown in the presence of arsenite. These experiments also showed an induction of several genes of the *norEFCBQD* nitric oxide reductase gene cluster when *Rhizobium* sp. NT-26 was grown in the presence of As(III) (table 1). These genes encode proteins that catalyze the reduction of nitric oxide to nitrous oxide, that is, *norQ, norE* and *norC* coding for a protein involved in nitric oxide reduction, a nitric oxide reductase activating protein, and the small subunit of the nitric oxide reductase, respectively. This suggests that the chemolithoautotrophic bacterium *Rhizobium* sp. NT-26 may fix CO_2 and couple nitrite reduction with As(III) oxidation. However, as no growth was observed with arsenite on either nitrate or nitrite, arsenite oxidation using nitrite as electron acceptor in autotrophic conditions seems unable to support sufficient energy (ATP) generation to sustain growth.

Rhizobium sp. NT-26 has been shown to grow with hydrogen sulfide, elemental sulfur, and thiosulfate (Santini J.M., unpublished data). In agreement with these observations, a *sox* cluster implicated in the oxidation of thiosulfate is present in the *Rhizobium* sp. NT-26 genome. Nevertheless, many genes involved in sulfur metabolism, that is, *soxGVWXYZ* and *cysT* were downregulated by up to 2-fold when the strain was grown in the presence of arsenite (table 1). Our results therefore suggest that, even though *Rhizobium* sp. NT-26 may be able to grow by using sulfur as an electron donor, the strain represses sulfur oxidation when grown in the presence of As(III). One hypothesis may be that, in such a case, the strain expresses a repressor of the *sox* genes. Their products serve for the oxidation of thiosulfate to sulfate and the reaction intermediates, that is, sulfite, sulfide, and hydrogen sulfide, have been shown to inhibit arsenite oxidase activity (Lieutaud et al. 2010).

Physiological and Genetic Approaches: Flagellar Motility and Biofilm Formation

Flagellum Cascade Features

Rhizobium sp. NT-26 is motile by the means of two subterminal flagella (Santini et al. 2000). Genes involved in their biosynthesis are organized in a large chromosomal cluster of 55 genes showing a perfect synteny with those of *S. meliloti*. In this flagellar regulon, *visN* and *visR* form part of the master operon and encode the proteins forming the VisNR heterodimer that acts as a global transcriptional regulator. This master regulator activates the expression of genes located in the cascade that encode flagella, motor, and chemotaxis proteins (Sourjik et al. 2000). In *Rhizobium* sp. NT-26, microarray data showed that the expression of *fliF*, coding for the flagellum M-ring protein, was induced when the organism was grown in the presence of As(III) (table 1). Furthermore, proteomic data showed a 9.7- and 7.2-fold-increase in the accumulation of flagellin proteins Fla and FlaA, respectively (table 1). The expression of *qseB* was also induced when *Rhizobium* sp. NT-26 was grown in the presence of As(III). QseB has been shown to participate in the flagellum and motility bacterial regulatory network via a quorum-sensing mechanism. Indeed, in *E. coli*, *qseBC* expression enhances the transcription of flagellar genes in response to the auto-inducer by a direct binding of QseB to the *flhDC* master operon promoter (Clarke and Sperandio 2005). Finally, microarray data showed the induction of genes possibly involved in the synthesis of an exopolysaccharide matrix in *Rhizobium* sp. NT-26, that is, *noeJ*, coding for a mannose-1-phosphate guanylyltransferase and *kdsA*, coding for a 2-dehydro-3-deoxyphosphooctonate aldolase. These observations suggest that As(III) has an impact on flagellum synthesis, that is to say motility, and biofilm formation in *Rhizobium* sp. NT-26, as observed in *H. arsenicoxydans* (Muller et al. 2007; Marchal et al. 2010). To test this hypothesis, swarming assays were performed on 0.3% agar plates. The presence of As(III) was shown to increase the swarming ring by up to 2-fold in the presence of 8 mM As(III) (fig. 4A). Remarkably, cell observation under a TEM revealed that flagellum biosynthesis occurred immediately in the presence of 8 mM As(III) while more than two days were needed to observe flagella in the absence of arsenite (fig. 4B and C), providing evidence that arsenite promotes motility in *Rhizobium* sp. NT-26. In addition, a two-fold reduction in biofilm formation was observed in the first 24 h of growth in the presence of As(III) (fig. 4D), which suggests a preferential development as motile planktonic cells rather than as unflagellated sessile cells as in *H. arsenicoxydans* (Marchal et al. 2010).

Random Mutagenesis

The *Rhizobium* sp. NT-26 genome organization suggests that motility and arsenite oxidation depend on genes located on its
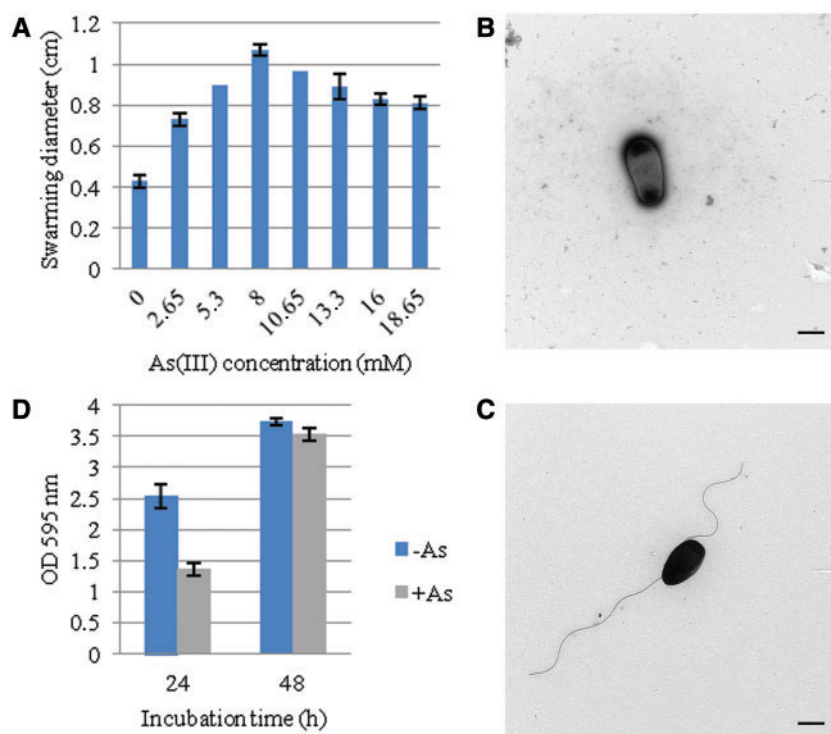
F𝗂𝗀. 4.—Motility phenotype of *Rhizobium* sp. NT-26 grown at different concentration of arsenite. (*A*) Swarming diameter measured after 48 h in MSM containing 0.04% yeast extract and supplemented by different concentrations of As(III). Results are the mean values of three independent experiments. (*B*) and (*C*) TEM observations of *Rhizobium* sp. NT-26 at 24 h of culture, without or with 8 mM As(III), respectively. The scale bar corresponds to 500 nm and the pictures are representative of 10 pictures. (*D*) Biofilm formation by strain NT-26, without or with 8 mM As(III) visualized by the crystal violet method. Results are the mean values of 24 replicates.

chromosome and on its megaplasmid, respectively. With the aim to analyze the possible link between these physiological processes, a mutant library was constructed by random transposon mutagenesis (Tang et al. 1999). The motility of 6,000 kanamycin-resistant transposition derivatives was tested on semisolid medium, which led to the isolation of 22 motility-deficient mutants. The mutations that resulted in a loss of motility were identified by sequencing the mini-Tn*5* transposon insertion sites. Fourteen mutations were shown to directly disrupt motility genes (table 2), and the proteins encoded by these genes are either structural or regulatory components of the flagellum cascade, that is, 5 Flg proteins (FlgE, FlgF, FlgG, FlgI, and FlgL), 5 Fli proteins (FliF, FliK, Flip, and FliR), 1 Flh protein (FlhA), and 1 Vis protein (VisR). No flagellin-defective mutant was obtained, which may be explained by the presence of four different flagellin-encoding genes on the chromosome.

Similarly, six mutations resulting in a lack of arsenite oxidation as compared with the wild-type and motility mutants were obtained after screening 6,000 kanamycin-resistant clones with the silver nitrate method (Muller et al. 2007) (table 2). First, two mutations were identified in the arsenite oxidase genes, that is, *aioA* and *aioB*. One

mutation was also shown to affect *aioR,* which encodes the regulatory protein of the AioRS two-component system. No oxidation of As(III) to As(V) was detected by HPLC-ICP-AES (Muller et al. 2007) in this mutant, as compared with complete As(III) oxidation determined in the motility mutant deficient in the flagellum master regulator VisR. A fourth mutation was located in the *moeB* gene involved in the synthesis of the molybdopterin cofactor required for arsenite oxidase activity. Finally, the inactivation of the *aioX* gene, which is located upstream of *aioSR*, also resulted in a loss of arsenite oxidation in *Rhizobium* sp. NT-26. In *A. tumefaciens* 5A, the periplasmic AioX has been recently shown to be involved in the regulation of As(III) oxidation (Liu et al. 2012).

To determine the link between As(III) oxidation and colonization properties in *Rhizobium* sp. NT-26, the ability of various mutants to move and to form a biofilm was evaluated in the presence of arsenite (fig. 5). Mutations in flagellar genes resulted in a loss of motility and in a decrease in biofilm formation. Indeed, all the mutants we tested were nonmotile (fig. 5A) and lost between 12% and 45% of their ability to form a biofilm when compared with the wild-type strain (fig. 5B). This observation demonstrates that, although

Table 2

Rhizobium sp. NT-26 Mutants Isolated on the Basis of a Loss of Motility or Arsenite Oxidation

Mutant	MaGe ID[a]	Gene	Function	Gene Location[b]	Insertion[c]
Motility					
2B5	NT26v4_0222	flgI	Flagellar P-ring protein precursor	221267–222391	258_{I-O}
2D6	NT26v4_0245	flhA	Flagellar biosynthesis protein	243262–245349	38_{I-O}
4H7	NT26v4_0204	fliF	Flagellar M-ring protein	206351–208027	477_{I-O}
5B7	NT26v4_0226	fliP	Flagellar biosynthetic protein	224272–225009	109_{O-I}
6E4	NT26v4_0220	flgG	Flagellar basal-body rod protein	219981–220769	182_{I-O}
10A11	NT26v4_0248		Putative FlgJ-like protein	246658–247212	
10G2	NT26v4_2965		Conserved hypothetical protein	2880029–2881285	44_{O-I}
16B6	NT26v4_0245	flhA	Flagellar biosynthesis protein	243262–245349	55_{I-O}
16B7	NT26v4_0240	flgL	Flagellar hook-associated protein	240428–241549	11_{I-O}
18D11	NT26v4_0238	flgE	Flagellar hook protein	237398–238930	363_{I-O}
20E7	NT26v4_0246	fliR	Flagellar biosynthetic protein	245378–246130	110_{O-I}
23E5	NT26v4_0214	flgF	Flagellar basal-body rod protein	216054–216788	44_{O-I}
29G6	NT26v4_0247		Putative FliR/FliJ-like chaperone	246137–246553	91_{I-O}
35A8	NT26v4_2314		Putative two-component sensor histidine kinase	2263060–2264472	113_{O-I}
37C12	NT26v4_2314		Putative two-component sensor histidine kinase	2263060–2264472	48_{O-I}
37H1	NT26v4_2267		Putative ATP-dependent hydrolase protein	2217585–2219546	337_{O-I}
38B4	NT26v4_0206	visR	Master transcriptional regulator of flagellar regulon	209070–209798	53_{O-I}
38G3	NT26v4_0204	fliF	Flagellar M-ring protein	206351–208027	235_{I-O}
39G12	NT26v4_2671		Conserved protein of unknown function	2586119–2587117	94_{O-I}
40E5	NT26v4_0234	fliK	Flagellar hook-length regulator	234324–235835	83_{I-O}
50E11	NT26v4_0250		Conserved integral membrane protein of unknown function	247603–248142	92_{O-I}
61C2	NT26v4_3970		Conserved exported protein of unknown function	3918374–3918853	196_{I-O}
Arsenite oxidation					
8G1	NT26v4_p10026	aioX	Putative periplasmic phosphite-binding-like protein precursor; PtxB-like protein	23892–24806	275_{I-O}
11B3	NT26v4_4048	moeB	Putative molybdopterin biosynthesis protein MoeB	3998958–3999725	245_{O-I}
24B7	NT26v4_p10028	aioR	Two-component response regulator	26262–27584	65_{I-O}
37C3	NT26v4_p10026	aioX	Putative periplasmic phosphite-binding-like protein precursor; PtxB-like protein	23892–24806	191_{I-O}
55H7	NT26v4_p10029	aioB	Arsenite oxidase small subunit	27721–28248	
60E6	NT26v4_p10030	aioA	Arsenite oxidase large subunit	28261–30798	818_{I-O}

[a]Identification number of the gene in the MaGe interface.
[b]Position of the corresponding gene on the chromosome or the plasmid.
[c]Position of the codon immediately upstream of the transposon insertion site. Subscripts indicate the orientation of the insertion.

Rhizobium sp. NT-26 has a preferential motile life style in the presence of arsenite, flagella have a role as adhesive appendages in the first steps of biofilm formation, which has been shown previously in other studies (Kirov et al. 2004; Nejidat et al. 2008). This result is in agreement with those obtained with H. arsenicoxydans, where mutations resulting in nonfunctional flagella led to a more rapid adhesion as compared with the wild-type. Finally, aioA and aioR mutants were less motile and formed 30% and 45%, respectively, less biofilm than the wild-type (fig. 5), further supporting the role of motility and flagella in biofilm formation.

Regulation of Flagella Synthesis by AioR

The "omics" data showed that flagellar proteins and genes were upregulated when strain NT-26 was grown in the presence of arsenite (table 1). Remarkably, both aioA and aioR mutations resulted in a moderate reduction in motility

(fig. 5A). This can be explained by the reduction in energy available to the cells as they are unable to metabolize arsenite (Santini et al. 2000). In addition, TEM observations of the aioR mutant, affected in the two-component signal transduction system, revealed the presence of flagella in the early log phase of growth even in the absence of As(III), which suggests that AioR may be involved in the repression of motility when no arsenite is present (fig. 6). AioR may thus interact, directly or indirectly, with components of the flagellar cascade.

To identify possible AioR-binding sites in the Rhizobium sp. NT-26 genome, multiple sequence alignments of all aioBA regulatory sequences available in databases were performed with fuzznuc (Rice et al. 2000). This enabled us to suggest the possible existence of two AioR putative binding sites upstream of the aioBA transcriptional start site, that is, GT[CT]CGN(6)CG[GA]AC in the Rhizobiales strains and GTTNCN(6)GNAAC in the Burkholderiales
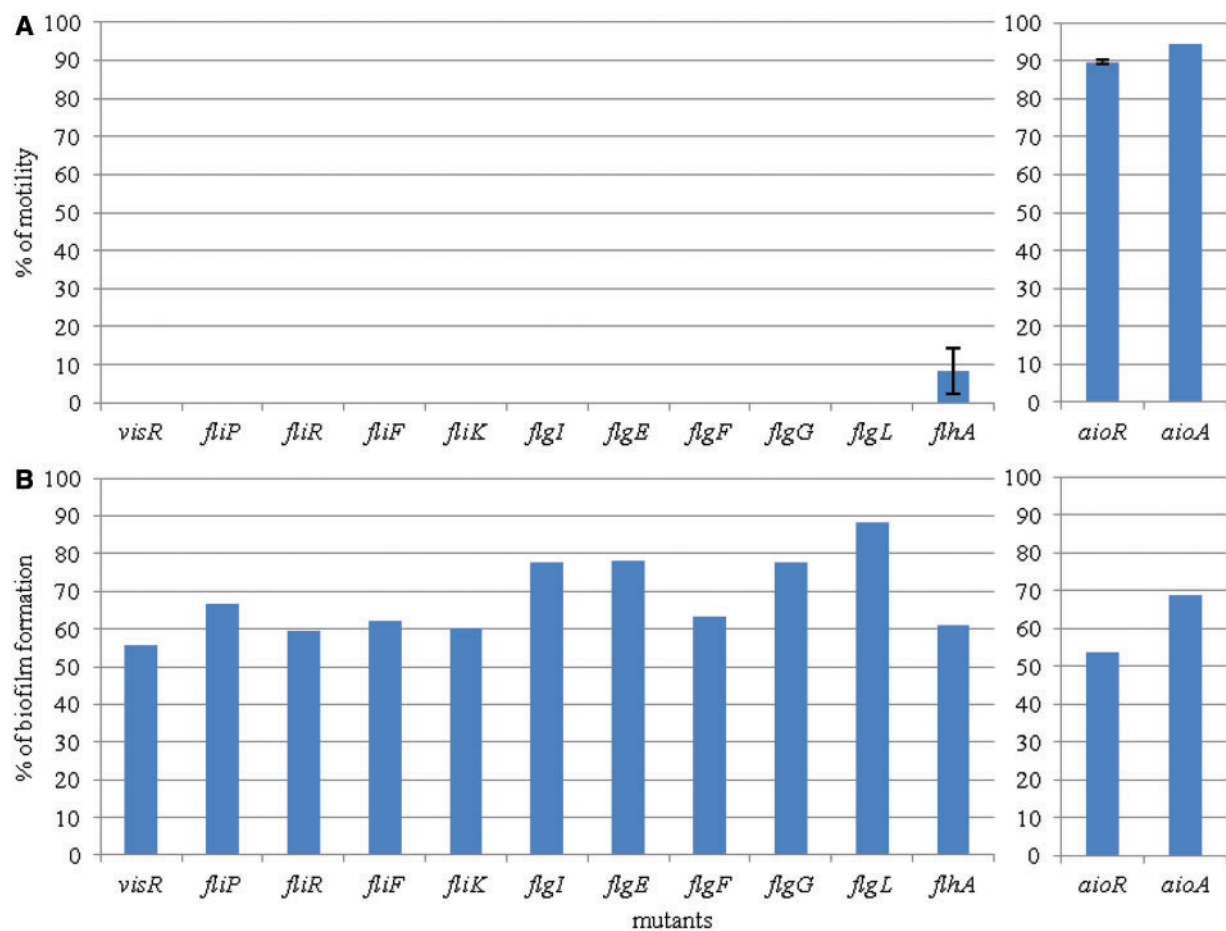
FIG. 5.—Percentage of motility and biofilm formation in various mutants as compared with *Rhizobium* sp. NT-26 wild-type strain. The left and the right panels show the results obtained in mutants affected in motility and As(III) oxidation, respectively. (A) % of swarming motility measured after 24 h. Results are the mean values calculated from the % of three independent experiments. In each experiment, mutant and wild-type strains were tested in triplicates. (B) % of biofilm formation visualized by crystal violet coloration. Results are the % calculated from the mean values of six replicates for each strain.

strains. In contrast, strains lacking the two-component system *aioSR* operon did not harbor any of these putative AioR-binding sites, which further supports a role for these motifs in the regulation of *aioBA* operon expression by AioR. Although the GT[CT]CGN(6)CG[GA]AC putative binding site was found at 49 locations on the *Rhizobium* sp. NT-26 chromosome, it is only in the upstream region of the *aioBA* operon that this motif was associated with the -12/-24 σ^{54}-dependent promoter sequence needed for the RpoN-dependent transcription initiation of arsenite oxidase genes (Koechler et al. 2010). Moreover, no clear connection could be observed between those putative binding sites and motility-related genes. Nevertheless, a search of the whole genome of strain NT-26 with a relaxed version of the pattern allowing any nucleotide at its degenerated positions, GTNCGN(6)CGNAC, yielded 39 more hits than with the canonical pattern. This low number of new hits suggests that the presence of this signature is not due to

chance and this sequence may therefore have a potential regulatory role. None of the new hits was associated with a RpoN motif site although one hit was found within the coding sequence of the flagellar master regulatory gene *visN*. Therefore, although we cannot rule out an indirect effect of AioR by controlling another regulatory protein, we can hypothesize that the binding to this mildly degenerate motif of unphosphorylated AioR in the absence of arsenic would result in a *visN* repression and a delayed motility. Such a transcriptional repression via binding of the coding sequence of target genes has already been observed for other regulatory proteins and two-component system regulators, for example, OxyR (Zheng et al. 2001) and PrrA (Eraso et al. 2008). Taken together, our results demonstrate the importance of arsenite oxidation in the behavioral response of *Rhizobium* sp. NT-26, suggesting that arsenic metabolism enhances the ability of the organism to explore and colonize its environment.
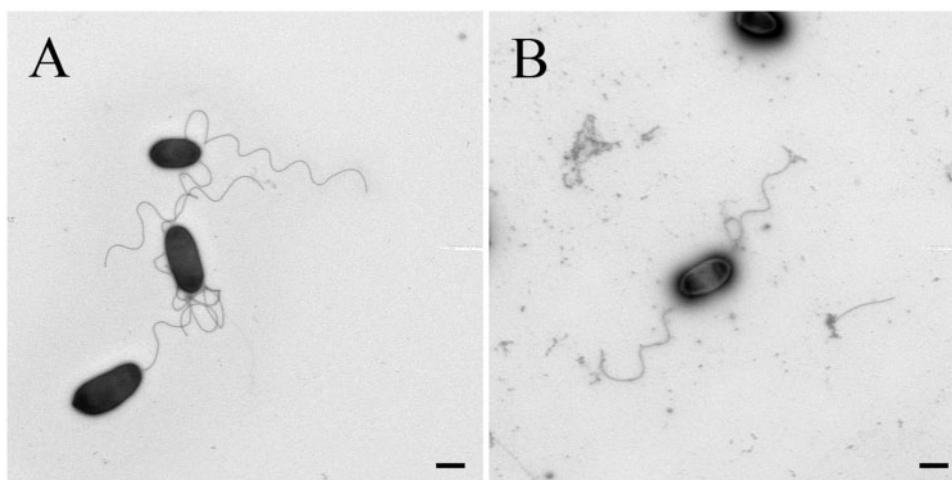
Fig. 6.—TEM observations of the *aioR* mutant. The *aioR* mutant was cultivated 24 h (*A*) in the absence of As(III) and (*B*) in the presence of 8 mM As(III). Pictures are representative of 10 photographs. The scale bar corresponds to 500 nm.
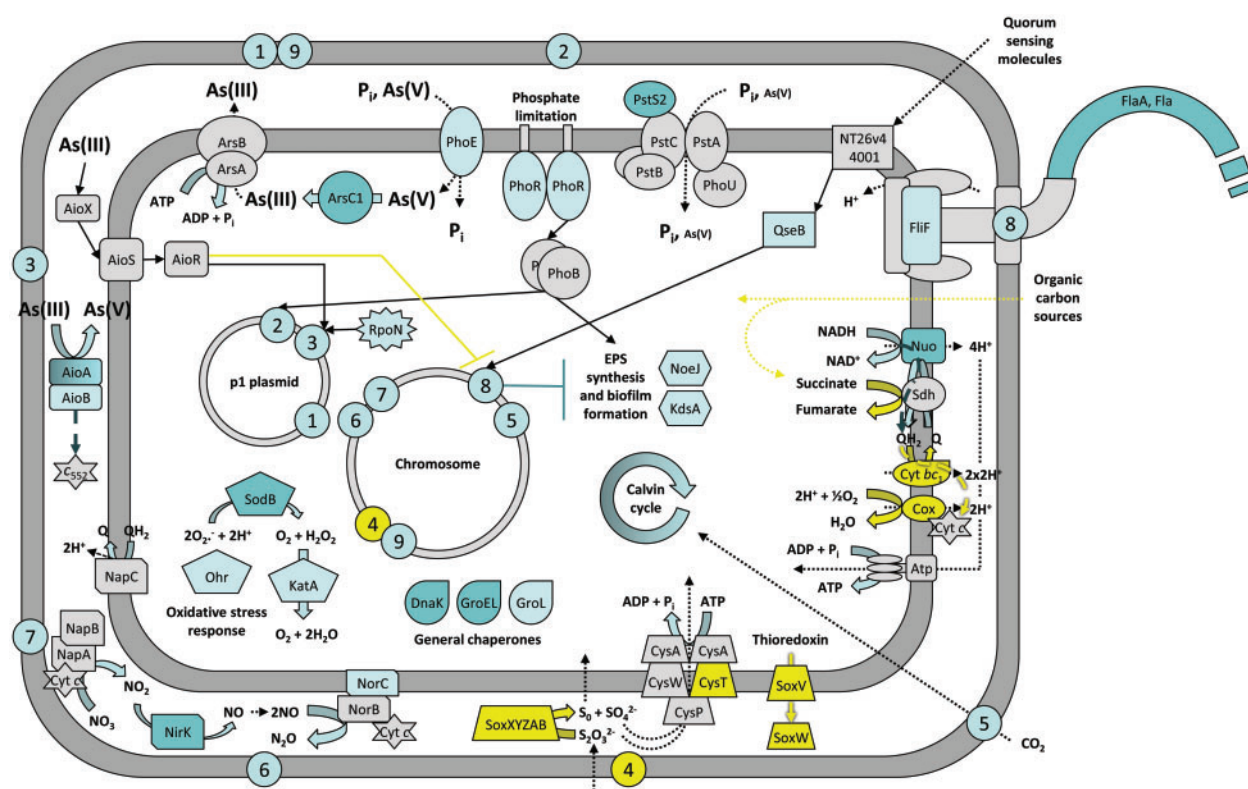

Fig. 7.—Conceptual representation of the *Rhizobium* sp. NT-26 response to arsenite exposure. This representation takes into account our genomic, transcriptomic, proteomic, and physiological results as well as data from the literature. Numbers 1 to 9 represent biological functions and the approximate genomic location of the gene clusters encoding their corresponding proteins. 1 and 9: arsenate reduction; 2: phosphate and arsenate transport; 3 and 4: arsenite and sulfur oxidation, respectively; 5: carbon fixation; 6 and 7: nitrate and nitrite reduction, respectively; 8: motility. Block, dashed, dotted, and standard arrows symbolize chemical reactions, electron flow, transport/utilization of molecules and signaling/regulatory pathways, respectively. When highlighted in dark blue, light blue, yellow or gray, elements have been identified as being induced by proteomic, induced by transcriptomic, repressed by transcriptomic, and present in the genome, respectively. For clarity reasons, proteins for which the exact function is still unknown but that are related to the different processes are not shown, the protein complexes of the respiratory chain, that is the NADH dehydrogenase, the fumarate reductase, the cytochrome bc_1 and the cytochrome c oxidase are designated by Nuo, Sdh, Cyt bc_1, and Cox, respectively, plasmid p2 is not shown and only one flagella is represented. Finally, Cyt c and c_{552} are for cytochrome c and cytochrome c_{552}, respectively, and NT26v4_4001 is a homolog of *qseC*.

Conclusion

This study extends our knowledge of the physiological response to arsenic in arsenite-oxidizing bacteria. Our results provide for the first time a reference set of genomic, transcriptomic, and proteomic data of an *Alphaproteobacterium* isolated from an arsenopyrite-containing goldmine, which allowed us to propose a model for the *Rhizobium* sp. NT-26 response to arsenite exposure (fig. 7). Although phylogenetically related to the plant-associated bacteria, strain sp. NT-26 has lost the major colonizing capabilities needed for symbiosis. Instead, this bacterium has acquired on a megaplasmid the various genes which allow it to metabolize arsenate. Remarkably, a link between flagellar motility/biofilm formation and arsenite oxidation was observed although the genes required for these physiological activities are carried by different genetic determinants, that is, the chromosome and the megaplasmid, respectively. This suggests the existence of a mechanism, probably indirect and which remains to be characterized at a molecular level, of a coordinate regulation of these two important biological processes. This underlines the importance of arsenite oxidation in the colonization of arsenic-rich ecosystems, a toxic element widespread on Earth. Importantly, our data also illustrate the major contribution of environmental pressure on the evolution of bacterial genomes, which results in a gain and loss of multiple functions, improving the fitness of the strains to extreme ecological niches.

Supplementary Material

Supplementary figures 1–4, tables S1–S6, and methods S1–S4 are available at *Genome Biology and Evolution* online (http://www.gbe.oxfordjournals.org/).

Acknowledgments

Literature Cited

Altschul SF, et al. 1997. Gapped BLAST and PSI-BLAST: a new generation of protein database search programs. Nucleic Acids Res. 25:3389–3402.

Arsène-Ploetze F, et al. 2010. Structure, function, and evolution of the *Thiomonas* spp. genome. PLoS Genet. 6:e1000859.

Aury J-M, et al. 2008. High quality draft sequences for prokaryotic genomes using a mix of new sequencing technologies. BMC Genomics 9:603.

Bernstam L, Nriagu J. 2000. Molecular aspects of arsenic stress. J Toxicol Environ Health B Crit Rev. 3:293–322.

Bertin PN, et al. 2011. Metabolic diversity among main microorganisms inside an arsenic-rich ecosystem revealed by meta- and proteogenomics. ISME J. 5:1735–1747.

Bertin PN, et al. 2012. Microbial arsenic response and metabolism in the genomics era. In: Santini JM, Ward SA, editors. The metabolism of arsenite. London: CRC Press. p. 99–114.

Bertin PN, Médigue C, Normand P. 2008. Advances in environmental genomics: towards an integrated view of micro-organisms and ecosystems. Microbiology 154:347–359.

Bigot T, Daubin V, Lassalle F, Perrière G. 2012. TPMS: a set of utilities for querying collections of gene trees. BMC Bioinformatics 14:109.

Borch T, et al. 2010. Biogeochemical redox processes and their impact on contaminant dynamics. Environ Sci Technol. 44:15–23.

Bradford MM. 1976. A rapid and sensitive method for the quantitation of microgram quantities of protein utilizing the principle of protein-dye binding. Anal Biochem. 72:248–254.

Branco R, Chung A-P, Morais PV. 2008. Sequencing and expression of two arsenic resistance operons with different functions in the highly arsenic-resistant strain *Ochrobactrum tritici* SCII24T. BMC Microbiol. 8:95.

Bryan CG, et al. 2009. Carbon and arsenic metabolism in *Thiomonas* strains: differences revealed diverse adaptation processes. BMC Microbiol. 9:127.

Carapito C, et al. 2006. Identification of genes and proteins involved in the pleiotropic response to arsenic stress in *Caenibacter arsenoxydans*, a metalloresistant beta-proteobacterium with an unsequenced genome. Biochimie 88:595–606.

Castresana J. 2000. Selection of conserved blocks from multiple alignments for their use in phylogenetic analysis. Mol Biol Evol. 17:540–552.

Clarke MB, Sperandio V. 2005. Transcriptional regulation of flhDC by QseBC and sigma (FliA) in enterohaemorrhagic *Escherichia coli*. Mol Microbiol. 57:1734–1749.

Cleiss-Arnold J, et al. 2010. Temporal transcriptomic response during arsenic stress in *Herminiimonas arsenicoxydans*. BMC Genomics 11:709.

Creus CM, et al. 2005. Nitric oxide is involved in the *Azospirillum brasilense*-induced lateral root formation in tomato. Planta 221:297–303.

Criscuolo A, Gribaldo S. 2010. BMGE (block mapping and gathering with entropy): a new software for selection of phylogenetic informative regions from multiple sequence alignments. BMC Evol Biol. 10:210.

Danhorn T, Hentzer M, Givskov M, Parsek MR, Fuqua C. 2004. Phosphorus limitation enhances biofilm formation of the plant pathogen *Agrobacterium tumefaciens* through the PhoR-PhoB regulatory system. J Bacteriol. 186:4492–4501.

Daubin V, Lerat E, Perrière G. 2003. The source of laterally transferred genes in bacterial genomes. Genome Biol. 4:R57.

Dénarié J, Debellé F, Promé JC. 1996. *Rhizobium* lipo-chitooligosaccharide nodulation factors: signaling molecules mediating recognition and morphogenesis. Annu Rev Biochem. 65:503–535.

Didelot X, Lawson D, Darling A, Falush D. 2010. Inference of homologous recombination in bacteria using whole-genome sequences. Genetics 186:1435–1449.

Dobbelaere S, Okon Y. 2007. The plant growth-promoting effect and plant responses. In: Elmerich C, Newton WE, editors. Associative and endophytic nitrogen-fixing bacteria and cyanobacterial associations. Nitrogen fixation: origins, applications, and research progress V. Dordrecht (The Netherlands): Springer. p. 145–170.

Edgar RC. 2004. MUSCLE: a multiple sequence alignment method with reduced time and space complexity. BMC Bioinformatics 5: 113.

Eraso JM, et al. 2008. Role of the global transcriptional regulator PrrA in *Rhodobacter sphaeroides* 2.4.1: combined transcriptome and proteome analysis. J Bacteriol. 190:4831–4848.

Gadd GM. 2010. Metals, minerals and microbes: geomicrobiology and bioremediation. Microbiology 156:609–643.

Gallie DR, Kado CI. 1988. Minimal region necessary for autonomous replication of pTAR. J Bacteriol. 170:3170–3176.

Giraud E, et al. 2007. Legumes symbioses: absence of *Nod* genes in photosynthetic bradyrhizobia. Science 316:1307–1312.

Gonzalez V, et al. 2006. The partitioned *Rhizobium etli* genome: genetic and metabolic redundancy in seven interacting replicons. Proc Natl Acad Sci U S A. 103:3834–3839.

Gouy M, Guindon S, Gascuel O. 2010. SeaView version 4: a multiplatform graphical user interface for sequence alignment and phylogenetic tree building. Mol Biol Evol. 27:221–224.

Gremaud MF, Harper JE. 1989. Selection and initial characterization of partially nitrate tolerant nodulation mutants of soybean. Plant Physiol. 89:169–173.

Guibaud G, van Hullebusch E, Bordas F. 2006. Lead and cadmium biosorption by extracellular polymeric substances (EPS) extracted from activated sludges: pH-sorption edge tests and mathematical equilibrium modelling. Chemosphere 64:1955–1962.

Guindon S, Delsuc F, Dufayard J-F, Gascuel O. 2009. Estimating maximum likelihood phylogenies with PhyML. Methods Mol Biol. 537:113–137.

Guindon S, Gascuel O. 2003. A simple, fast, and accurate algorithm to estimate large phylogenies by maximum likelihood. Syst Biol. 52: 696–704.

Hall-Stoodley L, Costerton JW, Stoodley P. 2004. Bacterial biofilms: from the natural environment to infectious diseases. Nat Rev Microbiol. 2: 95–108.

Hao Y, Charles TC, Glick BR. 2011. ACC deaminase activity in avirulent *Agrobacterium tumefaciens* D3. Can J Microbiol. 57:278–286.

Harrison PW, Lower RPJ, Kim NKD, Young JPW. 2010. Introducing the bacterial 'chromid': not a chromosome, not a plasmid. Trends Microbiol. 18:141–148.

Heinrich-Salmeron A, et al. 2011. Unsuspected diversity of arsenite-oxidizing bacteria as revealed by widespread distribution of the aoxB gene in prokaryotes. Appl Environ Microbiol. 77:4685–4692.

Holmes A, et al. 2009. Comparison of two multimetal resistant bacterial strains: *Enterobacter* sp. YSU and *Stenotrophomonas maltophilia* ORO2. Curr Microbiol. 59:526–531.

Hommais F, et al. 2002. Effect of mild acid pH on the functioning of bacterial membranes in *Vibrio cholerae*. Proteomics 2:571–579.

Hynes MF, McGregor NF. 1990. Two plasmids other than the nodulation plasmid are necessary for formation of nitrogen-fixing nodules by *Rhizobium leguminosarum*. Mol Microbiol. 4:567–574.

Janssen PJ, et al. 2010. The complete genome sequence of *Cupriavidus metallidurans* strain CH34, a master survivalist in harsh and anthropogenic environments. PLoS One 5:e10433.

Juhas M, et al. 2009. Genomic islands: tools of bacterial horizontal gene transfer and evolution. FEMS Microbiol Rev. 33:376–393.

Kang Y-S, Bothner B, Rensing C, McDermott TR. 2012. Involvement of RpoN in regulating bacterial arsenite oxidation. Appl Environ Microbiol. 78:5638–5645.

Katoh K, Toh H. 2008. Recent developments in the MAFFT multiple sequence alignment program. Brief Bioinform. 9:286–298.

Kirov SM, Castrisios M, Shaw JG. 2004. *Aeromonas flagella* (polar and lateral) are enterocyte adhesins that contribute to biofilm formation on surfaces. Infect Immun. 72:1939–1945.

Koechler S, et al. 2010. Multiple controls affect arsenite oxidase gene expression in *Herminiimonas arsenicoxydans*. BMC Microbiol. 10:53.

Lassalle F, et al. 2011. Genomic species are ecological species as revealed by comparative genomics in *Agrobacterium tumefaciens*. Genome Biol Evol. 3:762–781.

Le SQ, Gascuel O. 2008. An improved general amino acid replacement matrix. Mol Biol Evol. 25:1307–1320.

Lett M-C, Paknikar KM, Lièvremont D. 2001. A simple and rapid method for arsenite and arsenate speciation. In: Ciminelli VST, Garcia O Jr, editors. Biohydrometallurgy: fundamentals, technology and sustainable development, Part B. New York: Elsevier Science. p. 541–546.

Lieutaud A, et al. 2010. Arsenite oxidase from *Ralstonia* sp. 22. J Biol Chem. 285:20433–20441.

Liu G, et al. 2012. A periplasmic arsenite-binding protein involved in regulating arsenite oxidation. Environ Microbiol. 14:1624–1634.

López-Guerrero MG, et al. 2012. Rhizobial extrachromosomal replicon variability, stability and expression in natural niches. Plasmid 68: 149–158.

Marchal M, Briandet R, Koechler S, Kammerer B, Bertin PN. 2010. Effect of arsenite on swimming motility delays surface colonization in *Herminiimonas arsenicoxydans*. Microbiology 156:2336–2342.

Marchal M, et al. 2011. Subinhibitory arsenite concentrations lead to population dispersal in *Thiomonas* sp. PLoS One 6:e23181.

Marouga R, David S, Hawkins E. 2005. The development of the DIGE system: 2D fluorescence difference gel analysis technology. Anal Bioanal Chem. 382:669–678.

Martens M, et al. 2007. Multilocus sequence analysis of Ensifer and related taxa. Int J Syst Evol Microbiol. 57:489–503.

McDougald D, Rice SA, Barraud N, Steinberg PD, Kjelleberg S. 2012. Should we stay or should we go: mechanisms and ecological consequences for biofilm dispersal. Nat Rev Microbiol. 10:39–50.

Muller D, et al. 2007. A tale of two oxidation states: bacterial colonization of arsenic-rich environments. PLoS Genet. 3:e53.

Muller D, Lièvremont D, Simeonova DD, Hubert J-C, Lett M-C. 2003. Arsenite oxidase aox genes from a metal-resistant β-proteobacterium. J Bacteriol. 185:135–141.

Nejidat A, Saadi I, Ronen Z. 2008. Effect of flagella expression on adhesion of *Achromobacter piechaudii* to chalk surfaces. J Appl Microbiol. 105: 2009–2014.

Osborne TH, Santini JM. 2012. Prokaryotic aerobic oxidation of arsenite. In: Santini JM, Ward SA, editors. The metabolism of arsenite. London: CRC Press. p. 61–72.

Parvatiyar K, et al. 2005. Global analysis of cellular factors and responses involved in *Pseudomonas aeruginosa* resistance to arsenite. J Bacteriol. 187:4853–4864.

Penel S, et al. 2009. Databases of homologous gene families for comparative genomics. BMC Bioinformatics 10(6 Suppl):S3.

Ramírez-Bahena MH, Nesme X, Muller D. 2012. Rapid and simultaneous detection of linear chromosome and large plasmids in proteobacteria. J Basic Microbiol. 52:736–739.

Rice P, Longden I, Bleasby A. 2000. EMBOSS: the European Molecular Biology Open Software Suite. Trends Genet. 16:276–277.

Richardson AE, Barea J-M, McNeill AM, Prigent-Combaret C. 2009. Acquisition of phosphorus and nitrogen in the rhizosphere and plant growth promotion by microorganisms. Plant Soil. 321:305–339.

Rigaud J, Puppo A. 1975. Indole-3-acetic acid catabolism by soybean bacteroids. J Gen Microbiol. 88:223–228.

Ronquist F, et al. 2012. MrBayes 3.2: efficient Bayesian phylogenetic inference and model choice across a large model space. Syst Biol. 61:539–542.

Santini JM, et al. 2007. The NT-26 cytochrome c552 and its role in arsenite oxidation. Biochim Biophys Acta. 1767:189–196.

Santini JM, Sly LI, Schnagl RD, Macy JM. 2000. A new chemolithoautotrophic arsenite-oxidizing bacterium isolated from a gold mine: phylogenetic, physiological, and preliminary biochemical studies. Appl Environ Microbiol. 66:92–97.

Santini JM, vanden Hoven RN. 2004. Molybdenum-containing arsenite oxidase of the chemolithoautotrophic arsenite oxidizer NT-26. J Bacteriol. 186:1614–1619.

Sardiwal S, Santini JM, Osborne TH, Djordjevic S. 2010. Characterization of a two-component signal transduction system that controls arsenite oxidation in the chemolithoautotroph NT-26. FEMS Microbiol Lett. 313:20–28.

Slater SC, et al. 2009. Genome sequences of three Agrobacterium biovars help elucidate the evolution of multichromosome genomes in bacteria. J Bacteriol. 191:2501–2511.

Sourjik V, Muschler P, Scharf B, Schmitt R. 2000. VisN and VisR are global regulators of chemotaxis, flagellar, and motility genes in Sinorhizobium (Rhizobium) meliloti. J Bacteriol. 182:782–788.

Spaepen S, Vanderleyden J, Okon Y. 2009. Chapter 7: Plant growth-promoting actions of rhizobacteria. In: Van Loon LC, editor. Advances in botanical research, Vol. 51. Burlington: Academic Press. p. 283–320.

Stamatakis A. 2006. RAxML-VI-HPC: maximum likelihood-based phylogenetic analyses with thousands of taxa and mixed models. Bioinformatics 22:2688–2690.

Stolz JF. 2011. Microbial metal and metalloid metabolism: advances and applications, 1st ed. Washington DC: ASM Press.

Suyama M, Torrents D, Bork P. 2006. PAL2NAL: robust conversion of protein sequence alignments into the corresponding codon alignments. Nucleic Acids Res. 34:W609–W612.

Tang X, Lu BF, Pan SQ. 1999. A bifunctional transposon mini-Tn5gfp-km which can be used to select for promoter fusions and report gene expression levels in Agrobacterium tumefaciens. FEMS Microbiol Lett. 179:37–42.

Vallenet D, et al. 2006. MaGe: a microbial genome annotation system supported by synteny results. Nucleic Acids Res. 34:53–65.

Vallenet D, et al. 2009. MicroScope: a platform for microbial genome annotation and comparative genomics. Database (Oxford) 2009: bap021.

van Lis R, Nitschke W, Duval S, Schoepp-Cothenet B. 2012. Evolution of arsenite oxidation. In: Santini JM, Ward SA, editors. The metabolism of arsenite. London: CRC Press. p. 125–144.

van Lis R, Nitschke W, Duval S, Schoepp-Cothenet B. 2013. Arsenics as bioenergetic substrates. Biochim Biophys Acta. 1827: 176–188.

Weiss S, et al. 2009. Enhanced structural and functional genome elucidation of the arsenite-oxidizing strain Herminiimonas arsenicoxydans by proteomics data. Biochimie 91:192–203.

Wilkins MJ, et al. 2009. Proteogenomic monitoring of Geobacter physiology during stimulated uranium bioremediation. Appl Environ Microbiol. 75:6591–6599.

Wood DW, et al. 2001. The genome of the natural genetic engineer Agrobacterium tumefaciens C58. Science 294:2317–2323.

Young JM, Kuykendall LD, Martínez-Romero E, Kerr A, Sawada H. 2001. A revision of Rhizobium Frank 1889, with an emended description of the genus, and the inclusion of all species of Agrobacterium Conn 1942 and Allorhizobium undicola de Lajudie et al. 1998 as new combinations: Rhizobium radiobacter, R. rhizogenes, R. rubi, R. undicola and R. vitis. Int J Syst Evol Microbiol. 51:89–103.

Young JPW, et al. 2006. The genome of Rhizobium leguminosarum has recognizable core and accessory components. Genome Biol. 7: R34.

Zheng M, et al. 2001. Computation-directed identification of OxyR DNA binding sites in Escherichia coli. J Bacteriol. 183:4571–4579.

Zhong Z, et al. 2003. Nucleotide sequence based characterizations of two cryptic plasmids from the marine bacterium Ruegeria isolate PR1b. Plasmid 49:233–252.

Zumft WG. 1997. Cell biology and molecular basis of denitrification. Microbiol Mol Biol Rev. 61:533–616.

Associate editor: Purificación López-García